Article

Exploring the Mechanism of General Anesthesia: Kinetic Analysis of $GABA_A$ Receptor Electrophysiology

Daniel K. Lee,[1] Daniel J. Albershardt,[1] and Robert S. Cantor[1,2,*]
[1]Department of Chemistry, Dartmouth College, Hanover, New Hampshire; and [2]MEMPHYS Center for Biomembrane Physics, University of Southern Denmark, Odense, Denmark

ABSTRACT A kinetic model of the effect of agonist and anesthetics on ligand-gated ion channels, developed in earlier work, is further refined and used to predict traces observed in fast-perfusion electrophysiological studies on recombinant $GABA_A$ receptors under a wide range of agonist and/or anesthetic concentrations. The model incorporates only three conformational states (resting, open, and desensitized) but allows for the modulation of the conformational free energy landscape connecting these states resulting from adsorption of agonist and/or anesthetic to the bilayer in which the protein is embedded. The model is shown to reproduce the diverse and complex features of experimental traces remarkably well, including both anesthetic-induced and agonist-induced traces, as well as the modulation of agonist-induced traces by anesthetic, either coapplied or continuously present. The solutions to the kinetic equations, which give the time-dependence of each of the nine protein states (three ligation states for each of the three conformations), describe the flow of probability among these states and thus reveal the kinetic underpinnings of the traces. Many of the parameters in the model, such as the desorption rate constants of anesthetic and agonist, are directly related to model-independent experimental measurements and thus can serve as a definitive test of its validity.

INTRODUCTION

There is a broad consensus that inhalation anesthetics act by inhibiting the development of an action potential in postsynaptic membranes, and that they do so by modulating the activity of the membrane proteins that mediate synaptic neurotransmission. Although there is less agreement on specific protein targets, the most likely candidates are thought to be postsynaptic receptors, most of which are members of the cys-loop family of pentameric ligand-gated ion channels (pLGICs). However, the mechanism(s) by which small molecules with anesthetic potency influence receptor activity remain unknown. Indeed, it is not even known whether the anesthetic effect of many of these molecules occurs through direct binding to localized sites on receptors, or indirectly through adsorption to (and modulation of the physical properties of) the bilayer in which the receptors are embedded, or perhaps some combination of the two.

The difficulty in determining the molecular mechanism arises in large part because receptor activity is complex and incompletely understood. Fast-perfusion electrophysiological studies have explored the response of receptors to a pulse of their neurotransmitter agonist, which induces a conformational change that opens transmembrane channels through which selected ions can flow. (Rapid solution exchange provides a good experimental approximation of a "pulse" (boxcar) function, in which agonist concentration changes instantaneously from zero to some constant positive value at the beginning of the pulse, and returns instantaneously to zero at the end of the pulse.) For most receptors, single-channel measurements have revealed that the ion conductance in its open state(s) appears to be constant. For a patch containing a large number of receptors, the measured ion current is thus proportional to the fraction of channels in conducting states. The resulting current traces therefore provide, to within a multiplicative constant, the fraction of proteins in a conducting (open channel) conformation as a function of time. These traces can exhibit a remarkably complex time-dependence, the features of which may vary sensitively with agonist concentration. The degree of complexity increases in the presence of anesthetics, which modulate characteristic features of these traces in a manner that depends sensitively on anesthetic concentration.

The general class of mechanism by which anesthetics influence receptor activity can be categorized as either direct (binding to localized sites) or indirect (bilayer-mediated). However, neither the discovery of protein sites to which an anesthetic binds at clinical concentrations, nor (alternatively) an unambiguous determination that clinical concentrations of anesthetics modulate physical properties of lipid bilayers, would in itself provide a mechanistic understanding of anesthesia. Either way, a fundamental understanding additionally requires development of a detailed kinetic model that explicitly incorporates anesthetic effects (whether binding or bilayer-mediated), and that reproduces the complex kinetics of agonist-induced current traces and

Submitted October 30, 2014, and accepted for publication December 29, 2014.

*Correspondence: robert.cantor@dartmouth.edu

Editor: Kalina Hristova

0006-3495/15/03/1081/13 $2.00

http://dx.doi.org/10.1016/j.bpj.2014.12.052

the modulation of these traces by anesthetics over a wide range of both agonist and anesthetic concentrations. To be of any predictive value, such an approach must also be susceptible to model-independent experimental verification or falsification, which can thus serve to distinguish unambiguously between direct binding and bilayer-mediated models of anesthetic mechanisms. Although this may seem an obvious goal, a comprehensive kinetic model has not yet been suggested for a direct binding mechanism of action of inhalation anesthetics. This is perhaps surprising, given the current enthusiasm for a binding mechanism, the sophistication of fast-perfusion electrophysiological methods, and the availability of software through which numerical solutions can be obtained for classical kinetic schemes involving standard (Markovian) binding and conformational transitions.

For various members of the pLGIC family of receptors (predominantly $GABA_A$ and acetylcholine receptors), kinetic models have certainly been proposed to rationalize the experimentally observed response of the receptor to its agonist. The simplest models of $GABA_AR$ kinetics presume that the protein can exist in one of three conformational states: resting, open, and desensitized, in which only the open state conducts ions (1). The agonist interacts with the protein solely by binding to its pair of equivalent extracellular sites, which destabilizes the resting state relative to both the (kinetically favored) open state and the (thermodynamically favored) desensitized state. Such models can capture some of the general features of current traces, such as rapid activation followed by a gradual decrease in current (desensitization) in the continued presence of saturating concentrations of agonist. However, it is well known that they fail to reproduce the temporal complexity of experimental traces, particularly at high agonist concentrations (e.g., multiple timescales of desensitization) unless additional conformational states are added to the kinetic scheme. With the inclusion of such states and the appropriate adjustment of kinetic parameters, these kinetic models can indeed reproduce observed traces, albeit over limited ranges of concentration (2–7). However, aside from the improbability that a protein requires so many distinct conformational states for proper function, the value of such a model is limited, since the existence of those states cannot be confirmed experimentally. Furthermore, even with additional conformational states, such models are not able to reproduce traces over the broadest range of agonist concentration.

We have previously developed a general kinetic model (8) in which aqueous solutes (agonist and/or anesthetic) can adsorb to the bilayer, and thereby modulate the conformational free energy landscape of the protein. Although the model includes only the minimal set of three protein conformational states, this study shows that it can nonetheless reproduce the full range of complex features of electrophysiological traces. In brief, the complexity results from the time-dependence of solute adsorption to the bilayer, which modulates the rate constants of conformational transitions. As a first test, the model was shown (8) to provide excellent fits to data obtained for the special case in which currents were induced by volatile anesthetics alone (i.e., in the absence of agonist, which thus greatly simplifies the kinetic mechanism) in recombinant $\alpha_1\beta_2\gamma_{2L}$ $GABA_A$ receptors (9). Although this is a simpler special case, these fits provided values of parameters, such as bilayer adsorption and desorption rate constants of these anesthetics, which, in principle, could be directly compared with independent experimental measurements, and could thus serve as an unambiguous test of the model.

The next step is clearly to apply the full kinetic model developed in (8)—which includes binding of agonist to its canonical sites as well as adsorption of both agonist and anesthetics to the bilayer—to a set of experimental results for one (or preferably more) receptors. A conclusive test would require an extensive set of very accurate electrophysiological traces, in which concentrations of agonist and anesthetic(s) are independently and systematically varied over a wide range, up to concentrations far in excess of binding saturation of agonist and clinical values of anesthetics. Given its importance to the elucidation of anesthetic mechanisms, and more fundamentally to the mechanism of the complex agonist-induced behavior of receptors, it is surprising that such a comprehensive set of electrophysiological results simply does not exist in the literature for any one receptor. Validation of any kinetic model—whether based on direct binding of anesthetic or bilayer-mediated effects of both anesthetic and agonist—is extremely difficult in the absence of such data. Fortunately, however, many of the defining features of current traces are shared (at least qualitatively) by related receptor isoforms studied in different labs; these consistent features thus provide a sufficiently challenging test for any kinetic model. Of course, the model must not only be capable of reproducing observed traces, but its assumptions and architecture must be physically reasonable, and the values of any fitted parameters must also be susceptible to model-independent experimental confirmation.

We consider in this study the detailed characteristics of current traces through $GABA_A$ receptors, as these receptors have been extensively studied by fast-perfusion electrophysiological methods, and they have the advantage—common among inhibitory (anion-selective) receptors—that currents can be induced not only by agonists, but by supraclinical concentrations of anesthetics. To provide the most comprehensive test of the model, we examine predictions for three general classes of current traces, each over an extremely wide range of concentrations: anesthetic-induced (without agonist), agonist-induced (without anesthetic), and modification of agonist-induced traces by varying concentrations of anesthetic, either coapplied or continuously present.

MATERIALS AND METHODS

The general kinetic model was developed in Cantor et al. (8), hereafter labeled "I" to which the reader is referred for details; it is summarized in the next section, as well as in a recent review (10). All references to numbered equations and figures in Cantor et al. (8) are notated "I.xx," where xx is the equation or figure number. The subsequent section describes the further development of the approach, in which we have incorporated a set of additional approximations, which reduce significantly the number of independent kinetic parameters. This is followed by descriptions of the parameter set and methodology.

Kinetic model

The protein is assumed to exist in one of three conformational states: X = R (resting), D (desensitized), and O (open); only the open state is conducting. Conformational transitions among all three pairs of states are allowed; the desensitized state can thus be accessed from either the resting state (branched desensitization) or open state (linear desensitization). The two agonist binding sites are assumed to be equivalent, so that a protein in conformation X can exist in one of three ligation states $\{A_0X, A_1X, A_2X\}$, with appropriate statistical factors in the rate equations of binding and unbinding to account for the degeneracy of the monoliganded state. The kinetic scheme is shown in Fig. I.1 (i.e., Fig. 1 in (8)); for convenience, it has been provided as well in Fig. S1 in the Supporting Materials. The fraction of protein in state X with i bound agonist molecules is denoted $f_{A_iX}(t)$; because the fractions add to 1, the protein distribution is defined by any eight of these nine fractions. The kinetics of conformational transitions and the binding of agonist to protein sites are modeled using standard forms for the rate equations, expressed in terms of $f_{A_iX}(t)$, as detailed in Eqs. I.2 and I.3 (i.e., Eqs. 2 and 3 in (8)).

Each conformational state can be interpreted as a local minimum along a generalized conformational coordinate that describes the protein free energy landscape, as illustrated in Fig. I.2, and in Fig. 3 in (10). The landscape changes significantly upon binding of agonist. For example, with no agonist bound, the lowest free energy minimum is that of the resting state (A_0R), whereas for the diliganded protein, the free energy minima corresponding to the open and desensitized states (A_2O and A_2D) are both lower than that of the resting state (A_2R). Of course, the landscape describes not just the minima, but all points along the trajectories of conformational transitions, including the maxima associated with the barrier (activated complex) between each pair of conformational states. Free energy landscapes based on the parameter set used in this work are shown in Fig. S2 for both the unliganded and diliganded protein.

Adsorption of solutes (agonist or anesthetic) onto the lipid bilayer of the postsynaptic membrane alters the physical properties of the bilayer. The bilayer constitutes an important part of the fluid environment of the protein, so changes in bilayer physical properties can change the protein free energy, to a degree that may vary with position on the free energy landscape. The entire landscape, including the local minima (conformational states) and the maxima separating them, will thus be modulated nonuniformly by changes in bilayer properties, i.e., the free energy will change to a degree that varies with position along the conformational coordinate. Let x represent a generalized conformational coordinate and $G^\circ(x)$ the standard free energy landscape of the protein, where the standard state ($^\circ$) refers to the absence of any adsorbed solutes. In a Langmuir approximation, let θ_s represent the fractional bilayer adsorption of solute s (agonist or anesthetic), i.e., the fraction of its surface density at saturation. The free energy will vary with a sensitivity $\lambda_s(x)$ that depends both on location on the conformational landscape (x) and the identity of the solute. At low adsorption, the change will be proportional to θ_s, i.e.,

$$G(x) = G^\circ(x) + \theta_s \lambda_s(x). \quad (1)$$

Consider the effect of adsorption on the kinetics of a conformational transition $A_iX \rightarrow A_iY$ (i.e., from state X to state Y, with i ligands bound). Let $A_iXY^\ddagger$ represent the activated complex, at which the free energy reaches a maximum along the trajectory $A_iX \rightarrow A_iY$. To reasonable approximation, the transition rate constant $k_{A_iX\rightarrow A_iY}$ depends exponentially on $\Delta G^\ddagger$, the molar free energy barrier between the initial state ($x = A_iX$) and the activated complex ($x = A_iXY^\ddagger$), with

$$k_{A_iX\rightarrow A_iY} \propto \exp\{-\Delta G^\ddagger/RT\}, \quad (2)$$

and

$$\Delta G^\ddagger = G(A_iXY^\ddagger) - G(A_iX) = \Delta G^{\circ\ddagger} + \theta_s \Delta\lambda_{s,A_iX\rightarrow A_iY}, \quad (3)$$

where $\Delta\lambda_{s,A_iX\rightarrow A_iY} = \lambda_s(A_iXY^\ddagger) - \lambda_s(A_iX)$ represents the difference in sensitivities (to solute s) of the protein in the activated complex and in its initial state. If $\Delta\lambda_{s,A_iX\rightarrow A_iY} \neq 0$, then membrane adsorption/desorption of solute will cause k to vary with θ_s as in the following:

$$k_{A_iX\rightarrow A_iY} = k^\circ_{A_iX\rightarrow A_iY} \exp[-\theta_s \alpha_{s,A_iX\rightarrow A_iY}], \quad (4)$$

where k° represents the standard rate constant (i.e., at $\theta_s = 0$), and we define a dimensionless sensitivity of the rate constant: $\alpha_{s,A_iX\rightarrow A_iY} = \Delta\lambda_{s,A_iX\rightarrow A_iY}/RT$. Because adsorption/desorption of solutes does not occur instantaneously (i.e., θ_s varies with time), and because the exponential function can be such a sensitive function of its argument, the rate constants of conformational transitions are thus strongly time-dependent.

The time-dependence of adsorption, $\theta_s(t)$, is determined in a simple Langmuir approximation of adsorption/desorption kinetics, given in Eq. I.7. The equilibrium adsorption of solute at aqueous concentration c_s is thus (Eq. I.9):

$$\theta_{s,eq} = c_s K_{ads,s}/(1 + c_s K_{ads,s}),$$

where $K_{ads,s} = k_{on,s}/k_{off,s}$.

Additional approximations

The general model contains kinetic parameters that involve binding and unbinding of agonist to receptor, standard rate constants of transitions among conformational states for different degrees of ligation, the rate constants of adsorption/desorption to the bilayer for both agonist and anesthetic, and the sensitivities (described above) of rate constants of conformational transitions. Thermodynamic constraints reduce the number of independent parameters somewhat, as described by Eqs. I.12 to I.20. The physical principles inherent in the approximations of the model lead to additional relationships among both 1) the sensitivities and 2) the standard rate constants that further reduce the number of independent parameters, as follows.

Sensitivity parameters

Eq. I.18 indicates that the difference in sensitivities of the rate constants of opposing conformational changes is independent of ligation state:

$$\begin{aligned}\alpha_{s,A_0X\rightarrow A_0Y} - \alpha_{s,A_0Y\rightarrow A_0X} &= \alpha_{s,A_1X\rightarrow A_1Y} - \alpha_{s,A_1Y\rightarrow A_1X} \\ &= \alpha_{s,A_2X\rightarrow A_2Y} - \alpha_{s,A_2Y\rightarrow A_2X}, \quad (5)\end{aligned}$$

where {X,Y} = {R,O}, {O,D}, or {R,D}. These relations are exact, since they arise from thermodynamic constraints. As noted in Eq. I.19, each of these differences in the sensitivities of opposing rate constants is proportional to the difference in sensitivities of the free energies of the two states:

$$\alpha_{s,A_iX\rightarrow A_iY} - \alpha_{s,A_iY\rightarrow A_iX} = (\lambda_{s,A_iY} - \lambda_{s,A_iX})/RT. \quad (6)$$

The sensitivity λ_{s,A_iX} of the free energy of the state X to bilayer adsorption of a solute s presumably depends on the structural properties of the conformational state (shape, etc.) in the membrane domain. Since the binding of agonist A to conformational state X is presumed not to affect the structural properties of state X, it is thus reasonable to assume that the sensitivity of that state is independent of ligation, i.e.,

$$\lambda_{s,A_0X} = \lambda_{s,A_1X} = \lambda_{s,A_2X}. \quad (7)$$

This will presumably remain a good approximation at *any* point on the protein free energy landscape; not just at a local minimum (conformational state), but also at a maximum (activated complex), or anywhere else. The notation for the minima and maxima can thus be simplified to $\lambda_{s,X}$ and $\lambda_{s,XY^\ddagger}$, respectively. If so, then the difference in sensitivities of two different points on the protein free energy landscape will also be independent of ligation state. If the two points correspond to a pair of conformational states {X, Y}, then Eq. 7 simply regenerates the constraints given in Eq. 5 that arise from thermodynamic considerations. But if the two points on the free energy landscape correspond instead to a conformational state X and an adjacent transition state $XY^\ddagger$, then since

$$\alpha_{s,A_iX\to A_iY} = \left(\lambda_{s,XY^\ddagger} - \lambda_{s,X}\right)/RT, \quad (8)$$

it follows that the sensitivities of the rate constants are also independent of ligation state, i.e.,

$$\alpha_{s,A_0X\to A_0Y} = \alpha_{s,A_1X\to A_1Y} = \alpha_{s,A_2X\to A_2Y} = \alpha_{s,X\to Y} \quad (9)$$

For each solute *s*, this provides a set of 12 constraints, rather than just the six constraints given by Eqs. I.18 and I.19. There is one additional constraint relating opening, linear, and branched desensitization given by Eq. I.20, so that altogether only 18 – 13 = 5 independent sensitivity parameters remain for each solute.

Standard rate constants

The rate constants $k^\circ_{A_iX\to A_iY}$ are standard state values, in that they describe the kinetics of conformational transitions in the absence of solute adsorption to the bilayer. The thermodynamic constraints given by Eq. I.17 (one for each ligation state) reduce this number from 18 to 15. Unlike the sensitivities, these standard rate constants are strongly affected by ligation state (increased ligation shifts the equilibrium from the resting to the open and desensitized states). The equivalence of the two binding sites results in the two constraints given by Eq. I.15, which is expressed in terms of the rate constants in Eq. I.16. For example, for the opening/closing standard rate constants:

$$\frac{k^\circ_{A_2R\to A_2O}}{k^\circ_{A_2O\to A_2R}}\frac{k^\circ_{A_1O\to A_1R}}{k^\circ_{A_1R\to A_1O}} = \frac{k^\circ_{A_1R\to A_1O}}{k^\circ_{A_1O\to A_1R}}\frac{k^\circ_{A_0O\to A_0R}}{k^\circ_{A_0R\to A_0O}}. \quad (10)$$

Since the two ligand binding sites are equivalent, it is reasonable to assume further that the binding of a ligand alters the rate constant for a particular conformational transition by a constant multiplicative factor, i.e., independent of the number of ligands already bound. In other words, for each transition X→Y, a coefficient $v_{X\to Y}$ is defined such that

$$v_{X\to Y} = \frac{k^\circ_{A_2X\to A_2Y}}{k^\circ_{A_1X\to A_1Y}} = \frac{k^\circ_{A_1X\to A_1Y}}{k^\circ_{A_0X\to A_0Y}}, \quad (11)$$

and thus $k^\circ_{A_1X\to A_1Y} = \left(k^\circ_{A_0X\to A_0Y}k^\circ_{A_2X\to A_2Y}\right)^{1/2}$. This leaves 10 independent parameters for the standard rate constants: $\{k^\circ_{A_0X\to A_0Y}, k^\circ_{A_2X\to A_2Y}\}$ for any five of the six X→Y transitions. Note finally that the original constraints in Eq. I.16 are the ratio of the individual constraints for the opposing conformational transitions X→Y and Y→X. These two constraints can now be reexpressed to relate the agonist dissociation constants $K_{d,X}$ and $K_{d,Y}$ for a pair of states {X, Y}, where $K_{d,X} = k_{u,X}/k_{b,X}$, and thus

$$K_{d,O} = (v_{O\to R}/v_{R\to O})K_{d,R}, \quad (12)$$

$$\text{and} \quad K_{d,D} = (v_{D\to O}/v_{O\to D})K_{d,O}. \quad (13)$$

Parameter set

As described above, there are 10 independent parameters for the standard rate constants, and five independent sensitivity parameters for each solute. The six agonist binding/unbinding rate constants ($k_{b,X}$, $k_{u,X}$; X = {R, O, D}) are constrained by the two thermodynamic relations given in Eqs. 12 and 13, leaving four independent parameters. The adsorption (on-) and desorption (off-) rate constants for each solute ($k_{on,ag}$, $k_{off,ag}$; $k_{on,an}$, $k_{off,an}$) are unconstrained. The total number of independent parameters thus depends on which solutes are present. With both agonist and anesthetic, a total of 28 parameters need be specified; the number is reduced to 21 if only agonist is present. On the other hand, if only anesthetic is present, then since only the unligated state of the protein can exist, the diliganded standard rate constants and binding/unbinding parameters are eliminated, leaving only 12 independent parameters.

Fortunately, some of these parameters are directly related to specific characteristics of experimental traces. For example, the rate constants of binding/unbinding to the resting state {$k_{b,R}$, $k_{u,R}$}, the standard rate constant of opening from the diliganded resting state $k^\circ_{A_2R\to A_2O}$, and the associated equilibrium constant $K^\circ_{open,2} = k^\circ_{A_2R\to A_2O}/k^\circ_{A_2O\to A_2R}$ are determined from the dependence on agonist concentration of the shape of the current rise to its peak at the beginning of the pulse. Also, the fraction of protein in the open state at equilibrium in the absence of agonist has been estimated for various $GABA_A$ receptors (typically of order 0.01% to 0.1%), which thus constrains $K^\circ_{open,0} = k^\circ_{A_0R\to A_0O}/k^\circ_{A_0O\to A_0R}$, and the extent of desensitization at sufficiently high concentrations of agonist (high enough to ensure that the protein is essentially entirely diliganded, but not so high as to adsorb significantly to the bilayer) determines $K^\circ_{deslin,2} = k^\circ_{A_2O\to A_2D}/k^\circ_{A_2D\to A_2O}$. The equilibrium constant $K_{ads} = k_{on}/k_{off}$ of bilayer partitioning (adsorption/desorption) has been measured for various solutes, including anesthetics. As discussed elsewhere (10), the limited information available for transport-limited desorption rate constants of small solutes indicates that the range of values of k_{off} is fairly narrow—within an order of magnitude of 100 s^{-1}—for a surprisingly broad range of compounds.

Table 1 lists the parameter values used in the calculations reported in this article. They were chosen largely to reproduce the features of the current traces published in a series of papers (9,11–14) on the effects of inhalation anesthetics such as isoflurane on recombinant $\alpha_1\beta_2\gamma_{2L}$ $GABA_A$ receptors, over a broad range of agonist and isoflurane concentrations. Of the 28 parameters, the 14 constants of agonist binding and standard conformational transitions (columns 1 to 4 in Table 1) depend only on the protein and agonist; they are independent of any effects of bilayer adsorption and would thus need to specified for any model of agonist activation of receptors that includes both linear and branched desensitization. By contrast, the four constants involving bilayer adsorption {$k_{off,ag}$, $K_{ads,ag}$, $k_{off,an}$, $K_{ads,an}$} depend only on the solute (agonist or anesthetic) and the bilayer, i.e., they are independent of the protein. Only the 10 sensitivities ($\alpha_{s,X\to Y}$) depend both on the protein and on bilayer-mediated effects. Note that only three of the independent parameters {$K_{d,R}$, $K_{ads,ag}$, and $K_{ads,an}$} involve concentrations; the rest are either first-order rate constants or dimensionless.

An extended version of Table 1, containing additional (derived) parameters is given in Table S1. The effects of various representative levels of solute adsorption on the transition rate constants are shown in Table S2. Fig. S2 provides corresponding diagrams of the free energy landscapes for the unliganded and diliganded protein, with and without adsorbed solutes.

TABLE 1 Values of independent parameters

$K_{d,R}$	$k_{u,R}$	$k_{u,O}$	$k_{u,D}$	$k_{off,ag}$	$K_{ads,ag}^{-1}$	$k_{off,an}$	$K_{ads,an}^{-1}$
167 μM	100 s^{-1}	0.40 s^{-1}	4.0 s^{-1}	40 s^{-1}	10 mM	320 s^{-1}	2 mM
$K^{\circ}_{open,0}$	$K^{\circ}_{open,2}$	$k^{\circ}_{A_0R\to A_0O}$	$k^{\circ}_{A_2R\to A_2O}$	$\alpha_{ag,R\to O}$	$\alpha_{ag,O\to R}$	$\alpha_{an,R\to O}$	$\alpha_{an,O\to R}$
2.9×10^{-4}	30	8.1×10^{-4} s^{-1}	800 s^{-1}	6.0	−1.0	−9.1	−2.5
$K^{\circ}_{deslin,0}$	$K^{\circ}_{deslin,2}$	$k^{\circ}_{A_0O\to A_0D}$	$k^{\circ}_{A_2O\to A_2D}$	$\alpha_{ag,O\to D}$	$\alpha_{ag,D\to O}$	$\alpha_{an,O\to D}$	$\alpha_{an,D\to O}$
0.22	1.5	0.84 s^{-1}	1.1 s^{-1}	0.0	0.5	−0.4	10.7
		$k^{\circ}_{A_0R\to A_0D}$	$k^{\circ}_{A_2R\to A_2D}$	$\alpha_{ag,R\to D}$		$\alpha_{an,R\to D}$	
		5.4×10^{-3} s^{-1}	1.0 s^{-1}	6.4		−14.4	

Solution of kinetic equations

The time-dependent distribution of protein states is described by the fractions $\{f_{A_iX}(t)\}$. For a given parameter set, these are obtained from numerical solutions of the coupled differential equations given by Eq. I.2. In earlier work on anesthetic-induced traces (8), fits of the model to the experimental traces of Haseneder et al. (9) for long pulses of the anesthetics isoflurane and sevoflurane determined the parameters of the kinetic equations. For that (zero agonist) case, only three (A_0R, A_0O, and A_0D) of the nine protein states are populated, so the model simplifies considerably. It was found that the data could be fit by the model in the absence of any contribution from branched desensitization, i.e., if the desensitized state is only accessed by linear desensitization from the open state ($A_0O \rightleftarrows A_0D$). On the other hand, if access to the desensitized state were restricted to occur only from the resting state ($A_0R \rightleftarrows A_0D$), then it was found that some of the basic qualitative features of the traces could not be reproduced. In the work presented here, an analogous result was found for the case of agonist-induced traces (without anesthetic); they could also be fit very well with no contribution from the branched desensitization pathway (regardless of ligation), using identical values of the subset of parameters shared by the two cases. Additionally, for both cases, incorporation of both branched and linear desensitization resulted in equally good fits, but with different parameter sets. However, to reproduce the features of all *three* cases considered here (anesthetic modulation of agonist-induced traces as well as anesthetic- and agonist-induced traces) over the broadest possible range of solute concentrations, it was necessary to include both the branched and linear desensitization pathways; it could not be achieved with linear desensitization alone.

The measured current is proportional to the fraction of protein in an open conformation, irrespective of ligation, i.e., to $f_O(t) = f_{A_0O}(t) + f_{A_1O}(t) + f_{A_2O}(t)$. Because the numerical solution of the kinetic equations (Eq. I.2) provides the complete protein state distribution $\{f_{A_iX}(t)\}$ and its time derivatives, it gives a complete snapshot of the probability distribution and of the rate of flow of probability among these states at any moment, and thus elucidates the predominant kinetic pathways followed under various agonist/anesthetic conditions, and the origins of many of the characteristics of the traces. For example, as will be discussed below, it indicates under which conditions the desensitized state is accessed through the branched or linear paths, and the pathway followed from the diliganded desensitized state A_2D back to the unliganded resting state A_0R upon washout at the end of a pulse of agonist.

RESULTS

Three general types of current traces are considered: 1) anesthetic-induced (without agonist), 2) agonist-induced (without anesthetic), and 3) modification of agonist-induced traces by varying concentrations of anesthetic, either coapplied or continuously present. Because different researchers have studied $GABA_A$ receptors with a range of different subunit compositions, and using different electrophysiological methods, it is not surprising that published results differ substantially. We rely principally on a series of papers (9,11–15) that explored a broad range of concentrations both of agonist and of various inhalation anesthetics, including the very important case of anesthetic-induced traces. For a short pulse of agonist, they (and other groups) have also examined the effect of different modes of application of anesthetic: either coapplied with agonist or continuously present (13,16,17). Since predictions of bilayer-mediated and binding models of agonist effects differ substantially at extremely high agonist concentrations c_{ag}, we consider particularly the results of Mercik et al. (18), who explored this range of concentrations. A set of parameter values (Table 1) was determined that reproduces the features of all of these data. The predicted traces for each of the three general cases are considered sequentially. For each, the results are described for different ranges of concentrations, and for each concentration range, an overview of the kinetic underpinnings (the flow of protein probability) is described. This is complemented by animation software, provided in the Supporting Material, that dynamically illustrates the time-dependent flow of probability among all protein states in the kinetic scheme. It is run interactively, allowing the user to vary agonist concentration, anesthetic concentration, and pulse duration.

Anesthetic-induced currents

Fig. 1 *a* provides the response to a long (1.5 s) pulse of isoflurane for different values of anesthetic concentration c_{an} as predicted by the model using the parameters listed in Table 1. These traces can be compared with the results of Haseneder et al. (9), who studied the activation of recombinant $\alpha_2\beta_2\gamma_{2L}$ $GABA_A$ receptors in response to a 1.5 s pulse of the volatile anesthetics isoflurane and sevoflurane, each over a wide range of c_{an}. The features of the experimental traces are well reproduced by the model: specifically 1) the onset of the pulse and approach to equilibrium, and 2) the deactivation following the end of the pulse (i.e., upon washout of anesthetic).

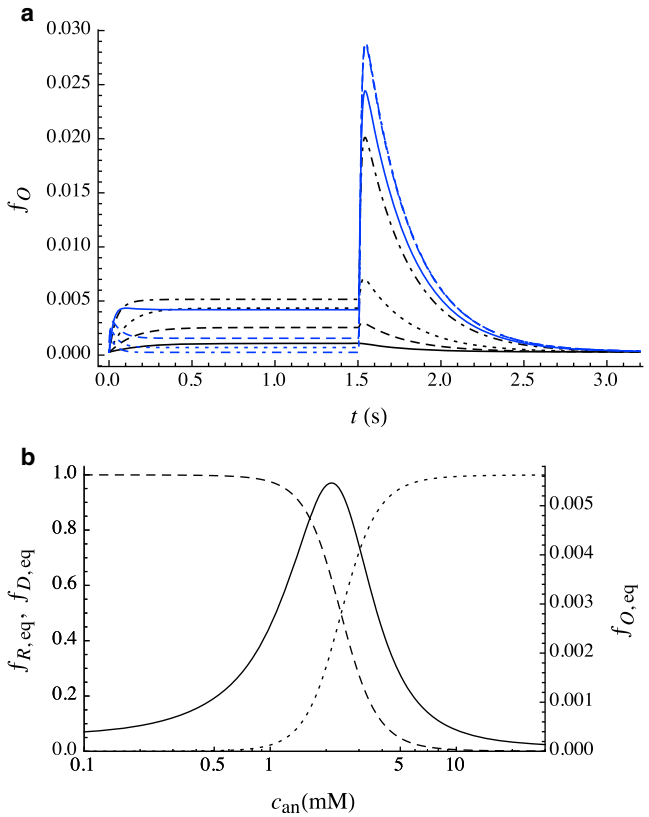

FIGURE 1 (*a*) Predicted open fraction $f_O(t)$ for a 1.5 s pulse of anesthetic for a wide range of concentrations: $c_{an} = 0.5$ mM (*black solid line*), 1.0 mM (*black dashed line*), 1.5 mM (*black dotted line*), 2.5 mM (*black dot-dashed line*), 3.0 mM (*blue solid line*), 5.0 mM (*blue dashed line*), 7.5 mM (*blue dotted line*), and 15.0 mM (*blue dot-dashed line*). (*b*) Equilibrium conformational distribution as a function of anesthetic concentration c_{an}: $f_{O,eq}$ (*solid line*), $f_{R,eq}$ (*dashed line*), and $f_{D,eq}$ (*dotted line*). Note the different scales for $f_{O,eq}$ (*right ordinate*) and for $f_{R,eq}$ and $f_{D,eq}$ (*left ordinate*). The shape of the distribution results from the increase in G(R) and the decrease in G(D) relative to G(O) upon bilayer adsorption of anesthetic. A key feature is the prediction of a very steep decrease in $f_{O,eq}$ after its maximum (i.e., for $c_{an} > c_{an,max} \approx 2$ mM) as observed experimentally (9), which is inconsistent with a mechanism based on anesthetic binding to a channel-blocking site. To see this figure in color, go online.

Onset of pulse

As discussed in detail by Cantor et al. (8), at low c_{an} the open fraction $f_O = f_{A_0O}$ rises monotonically and slowly to its equilibrium value $f_{O,eq}(c_{an})$. With increasing c_{an}, both the rate of the initial rise and the value of $f_{O,eq}$ increase, with $f_{O,eq}$ reaching a maximal value at concentration $c_{an,max}$ that is roughly an order of magnitude larger than the clinical concentration of isoflurane. For $c_{an} > c_{an,max}$, the initial rise in current continues to accelerate but the approach to the equilibrium value is no longer monotonic, with the value of $f_{O,eq}$ decreasing rapidly with increasing c_{an}; nearly to zero at roughly $5c_{an,max}$, as shown in Fig. 1 *b*.

This latter observation is very important, as this precipitous drop in $f_{O,eq}$ over only a fivefold increase in concentration is completely *inconsistent* with a "blocking" mechanism, i.e., the binding of the anesthetic to a putative site that blocks the flow of ions through the channel. In addition, the rate of acceleration of the initial rise with increasing c_{an} is also far greater than would be predicted by a simple binding model. Haseneder et al. (9) and Hapfelmeier et al. (13) modeled these current traces by including a kinetic step of binding to a site that blocks ion flow through the channel, but a comparison of predicted and experimental equilibrium currents at $c_{an} = 15$ mM in Figs. 4a and 6b in Haseneder et al. (9) shows that the agreement is poor at the highest concentrations.

Even for this relatively simple case (no agonist), the flow of protein probability is complex. Initially, almost all of the protein is in the resting state, with extremely low rate constants (and thus negligibly slow kinetics) of the conformational transitions to either the open or desensitized state; both are of order 10^{-3} s^{-1}. Upon introduction of anesthetic in the aqueous phase (assuming rapid solution exchange), equilibration with the bilayer occurs on a timescale of order $(k_{off,an} + c_{an}k_{on,an})^{-1}$. The predicted desorption rate constant for isoflurane is high enough ($k_{off,an} = 320$ s^{-1}) that the approach to adsorption equilibrium is essentially complete in less than 10 ms. Because the values of $\alpha_{an,R\to O} = -9.1$ and $\alpha_{an,R\to D} = -14.4$ are negative, anesthetic adsorption significantly accelerates both opening ($A_0R \rightarrow A_0O$) and branched desensitization ($A_0R \rightarrow A_0D$), but to a far greater extent for the latter than the former. Except at high c_{an}, which is considered below, the increase in these transition rate constants from their values in the absence of anesthetic to their equilibrium values at c_{an} is essentially complete before the resulting flow of protein probability has begun, so the two conformational transitions occur essentially under the influence of the rate constants at equilibrium adsorption. For the reverse processes ($A_0D \rightarrow A_0R$ and $A_0O \rightarrow A_0R$), since the magnitudes of both $\alpha_{an,O\to R}$ ($= -2.5$) and $\alpha_{an,D\to R}$ ($= +3.3$) are relatively small, the rate constants of both of these reverse processes change far less upon adsorption of anesthetic than do the rate constants for $A_0R \rightarrow A_0D$ and $A_0R \rightarrow A_0O$. The equilibrium thus shifts from the resting state toward both the open and desensitized states, but unequally, increasingly favoring the desensitized state at higher c_{an}. With increasing c_{an}, the increase in $K_{open,0}(= k_{A_0R\to A_0O}/k_{A_0O\to A_0R})$ results in the development of a small current, but the concomitant, and far larger increase in $K_{desbr,0}(= k_{A_0R\to A_0D}/k_{A_0D\to A_0R})$ causes an increasing fraction of protein to go directly to the desensitized state.

As c_{an} reaches and exceeds $c_{an,max}$, branched desensitization becomes so rapid that it competes with adsorption, and thus the flow of protein probability begins before $k_{A_0R\to A_0D}$ has reached its equilibrium value. The result is that the initial flow into the open state over the first few milliseconds generates an open fraction the exceeds its equilibrium value: the ultimate rise of $k_{A_0R\to A_0D}$ to its equilibrium value reduces f_R nearly to zero, inducing a net flow from A_0O to

A_0D via the A_0R state, i.e., $A_0O \rightarrow A_0R \rightarrow A_0D$. The timescale of flow through these two sequential steps is determined by the slower rate constant ($k_{A_0O \rightarrow A_0R}$). Because $\alpha_{an,O \rightarrow R} < 0$, $k_{A_0O \rightarrow A_0R}$ increases with c_{an}, and the decrease of current (after it passes through its maximum near the beginning of the pulse) to its equilibrium value occurs more rapidly with increasing c_{an}.

Deactivation

As observed experimentally, a "rebound" current is predicted to occur within a few tenths of a second upon washout, the magnitude of which (unlike the equilibrium reached during the pulse) increases monotonically with increasing c_{an}; it approaches a maximum at concentrations not much higher than $c_{an,max}$. The rapid washout of anesthetic (on the submillisecond timescale) causes desorption of anesthetic from the bilayer, which occurs on the timescale of a few milliseconds ($k_{off,an} = 320\ s^{-1}$) as discussed above. At lower levels of bilayer adsorption, the conformational transition rate constants are sufficiently low that they occur on a much slower timescale than anesthetic desorption, and thus the relaxation back to the zero-absorption equilibrium is well described as occurring under the influence of the standard (zero-absorption) rate constants $k^{\circ}_{A_0X \rightarrow A_0Y}$. For low c_{an}, $f_{D,eq}$ is small, so the dominant process upon washout is $A_0O \rightarrow A_0R$, and there is thus no rebound peak. At higher c_{an}, an increasing fraction of protein is in the A_0D state at the end of the pulse, and it is the return from A_0D to A_0R via A_0O, i.e., $A_0D \rightarrow A_0O \rightarrow A_0R$, that is responsible for the rebound current. Because $k^{\circ}_{A_0D \rightarrow A_0R}$ ($\approx 85\ s^{-1}$) >> $k^{\circ}_{A_0D \rightarrow A_0O}$ ($\approx 3.8\ s^{-1}$), the dominant path out of the A_0D state is directly to A_0R, so even if all the protein is in the A_0D state at the beginning of washout, the rebound peak remains small ($f_O \approx 0.03$). The height of the rebound peak thus varies with $f_{D,eq}$, which in turn is a very strong function of c_{an}, as shown in Fig. 1 *b*. The peak in the rebound is reached in a time determined by the rate of depletion of A_0D: as f_D drops and f_O rises, the rate of the $A_0D \rightarrow A_0O$ step decreases compared with $A_0O \rightarrow A_0R$, and the subsequent decay of the rebound peak occurs on a timescale determined by $k^{\circ}_{A_0O \rightarrow A_0R} \approx 2.8\ s^{-1}$.

Agonist-induced currents

Current traces evoked by a long pulse of agonist have been obtained experimentally for $GABA_A$ receptors, although generally only for a limited range of agonist concentrations. Although the details vary among experimental groups, the dependence of the qualitative features of these traces on c_{ag} are reasonably consistent and are reproduced by the predicted traces as shown in Fig. 2. Since $K_{d,R}$ (the agonist dissociation constant for the resting state) varies widely among $GABA_A$ receptor isoforms, values of c_{ag} are expressed in terms of $K_{d,R}$. These features are described below, for progressively higher c_{ag}; they are readily interpreted in the context of our kinetic model.

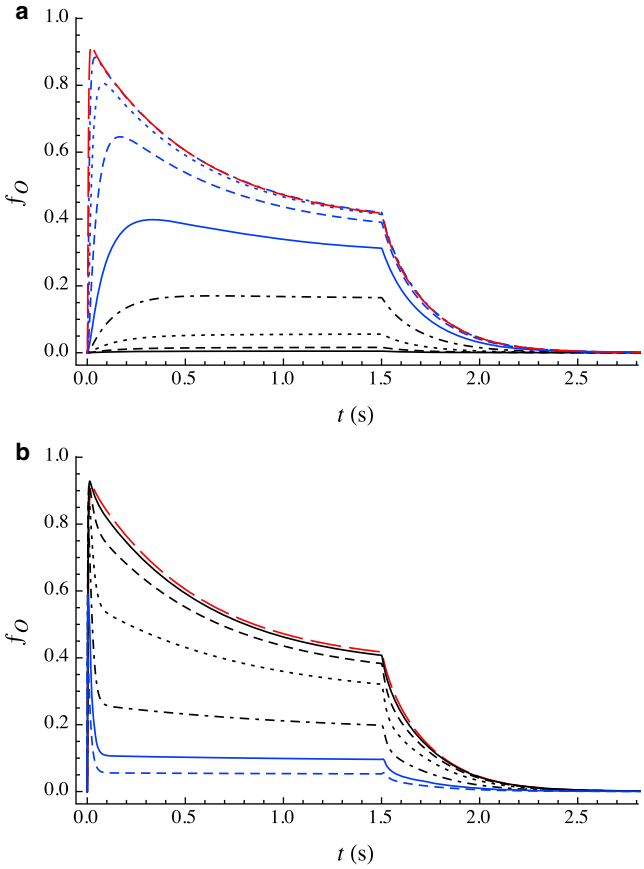

FIGURE 2 Predicted open fraction $f_O(t)$ for a 1.5 s pulse of agonist over a wide range of concentrations (expressed relative to $K_{d,R} = 167\ \mu M$) in equal multiplicative increments of $10^{1/3} = 2.154$. (*a*) $c_{ag}/K_{d,R} = 0.01$ (*black line*), 0.02154 (*black dashed line*), 0.04642 (*black dotted line*), 0.1 (*black dot-dashed line*), 0.2154 (*blue line*), 0.4642 (*blue dashed line*), 1 (*blue dotted line*), 2.154 (*blue dot-dashed line*), and 4.642 (*red long dashed line*). (*b*) $c_{ag}/K_{d,R} = 4.642$ (*red long dashed line*), 10 (*black line*), 21.54 (*black dashed line*), 46.42 (*black dotted line*), 100 (*black dot-dashed line*), 215.4 (*blue line*), 464.2 (*blue dashed line*), and 1000 (*blue dotted line*). To see this figure in color, go online.

Very low c_{ag}

Note first that the binding affinity is predicted to be more than two orders of magnitude weaker for the R state than for either the O or D states. Upon agonist binding, the O state is kinetically favored ($k^{\circ}_{A_2R \rightarrow A_2O} \gg k^{\circ}_{A_2R \rightarrow A_2D}$ or $k^{\circ}_{A_2O \rightarrow A_2D}$), but the D state is thermodynamically favored ($K_{d,D} < K_{d,O} \ll K_{d,R}$). Currents begin to be observed for c_{ag} ~$10K_{d,O}$. For sufficiently low c_{ag} (~$50K_{d,O}$) such that the current reaches no more than perhaps 20% of its maximum value, little functional desensitization is observed: f_O rises monotonically and slowly to its steady-state value. This plateau arises from sequential kinetics: upon binding of the first agonist molecule to the R state ($A_0R + A \rightarrow A_1R$), the subsequent shift in conformational distribution toward the desensitized state is essentially entirely a slow transfer in two parts: $A_1R \rightarrow A_2O \rightarrow A_2D$. (The direct path from R to D, branched

desensitization, is sufficiently slow that it makes no appreciable contribution.) The predominant path for the first part ($A_1R \rightarrow A_2O$) depends on the details of the parameter values, and can favor either $A_1R + A \rightarrow A_1O + A \rightarrow A_2O$ or $A_1R + A \rightarrow A_2R \rightarrow A_2O$.

Note that although f_O reaches its steady-state value within ~0.5 s, the system has not yet reached equilibrium. Because the rate constants of linear desensitization and resensitization are both small, the net transfer from A_1R to A_2D is slow. Thus, it takes far longer to attain the equilibrium values of the fractions of protein in all nine of the conformational/ligation states than it does to reach the steady-state current.

$c_{ag} \sim K_{d,R}$

Slow desensitization begins to be observed on a single timescale as c_{ag} is increased (but still sufficiently less than $K_{d,R}$ such that the peak current is well below its maximum value). The extent of desensitization increases with c_{ag}, correlating with an increase in the fraction in the open state at its peak. With increasing c_{ag}, as the value of the peak current reaches its maximum, desensitization remains slow and well approximated by a single exponential. Over this range of concentrations, the observed desensitization is entirely a result of a transition from the O to the D state, predominantly in the diliganded form at higher c_{ag}. Also, with increasing c_{ag} the peak current is reached increasingly rapidly, indicating that binding of a pair of ligands to the R state (rather than the subsequent $A_2R \rightarrow A_2O$ step) remains rate-limiting.

Deactivation is complex. At the end of the pulse, almost all of the protein is in either the A_2O or A_2D states; we consider their fates separately. A_2O is straightforward: the dominant path is $A_2O \rightarrow A_2R \rightarrow 2A + R$. A_2D is more complex: unbinding of the first ligand ($A_2D \rightarrow A + A_1D$) is predicted to dominate both of the conformational transitions ($A_2D \rightarrow A_2O$ or $A_2D \rightarrow A_2R$), whereas A_1D undergoes both further ligand unbinding and $A_1D \rightarrow A_1O$ ($\rightarrow A_1R$) at competitive rates. As a result, although the decay of $f_{A_2O}(t)$ is approximately exponential, $f_{A_1O}(t)$ rises through a small maximum and then decays (more slowly), so that $f_O(t)$ is not well fit by a single exponential during deactivation.

$c_{ag} > K_{d,R}$

An initial fast component of functional desensitization is observed, the extent of which increases with c_{ag} at values well in excess of $K_{d,R}$. The subsequent slow desensitization has time constant similar to that observed at lower c_{ag}. In the context of our model, the decrease in f_O associated with the fast component of desensitization is not caused by an increase in f_D, but rather by a shift in the $A_2R \rightleftarrows A_2O$ equilibrium back from the open to the resting state, i.e., an increase in f_R. This reequilibration results from bilayer adsorption of agonist, which alters the rate constants of opening and closing unequally: opening is slowed ($\alpha_{ag,R\rightarrow O} \approx 6$) with little effect on closing ($\alpha_{ag,O\rightarrow R} \approx -1$). At these saturating concentrations of agonist, the adsorption-induced changes in rate constants occur on a timescale that is significantly slower than the rapid initial rise to the peak current, which follows the sequential mechanism $2A + R \rightarrow A + AR \rightarrow A_2R \rightleftarrows A_2O$. The timescale of binding is of order $(c_{ag}k_{b,R})^{-1}$, whereas the timescale of equilibration of the final pair of reversible opening/closing steps is of order $(k^\circ_{A_2R\rightarrow A_2O} + k^\circ_{A_2O\rightarrow A_2R})^{-1} \approx k^\circ_{A_2R\rightarrow A_2O}{}^{-1}$. Thus, for $c_{ag} < k^\circ_{A_2R\rightarrow A_2O}/k_{b,R}$, binding is rate-limiting, whereas for $c_{ag} > k^\circ_{A_2R\rightarrow A_2O}/k_{b,R}$, channel opening is rate-limiting. So, in this concentration range (particularly at higher c_{ag}) the formation of the peak occurs in a few milliseconds, which is an order of magnitude faster than the predicted timescale of equilibration of agonist adsorption: $(k_{off,ag} + c_{ag}k_{on,ag})^{-1} \approx k_{off,ag}{}^{-1} = 0.025$ s. The peak current is thus reached before effects of adsorption become significant.

For many $GABA_A$ receptors, the timescale of the slow component of functional desensitization has been observed to remain fairly independent of c_{ag} (4,5,15) even as c_{ag} is raised to values at which significant fast desensitization occurs (resulting, in the context of our kinetic model, from bilayer adsorption of agonist). The rate of slow desensitization is determined by $k_{slow\ des} = k_{A_2O\rightarrow A_2D} + k_{A_2D\rightarrow A_2O}$. Because both of these rate constants are little changed from their standard values, the corresponding sensitivities, $\alpha_{ag,O\rightarrow D}$ and $\alpha_{ag,D\rightarrow O}$, must be zero, or nearly so. In other words, the part of the free energy landscape connecting the O and D states is unaffected by agonist adsorption.

Deactivation is more complex than at the somewhat lower concentrations described in the previous section (binding saturation, but without adsorption) because of the modulation of rate constants during the first few hundredths of a second of washout, as agonist desorbs from the bilayer: this is the origin of the steep initial decay.

$c_{ag} >> K_{d,R}$

Adsorption of agonist to the bilayer occurs on a timescale $(c_{ag}k_{on,ag})^{-1}$. At extremely high values of c_{ag}, significant adsorption thus occurs before equilibration of A_2R and A_2O. Since adsorption of agonist slows the $A_2R \rightarrow A_2O$ transition (while slightly accelerating the $A_2O \rightarrow A_2R$ transition) the equilibrium shifts toward the closed state, and the peak open fraction thus decreases with increasing c_{ag}. The onset of this effect has been observed by various groups that have explored current traces at high c_{ag} (4,15), but most strikingly by Mercik et al. (18) who obtained traces in response to agonist concentration in the 10 to 100 mM range. This mechanism also predicts the observed reduction in the equilibrium open fraction $f_{O,eq}$ (i.e., after slow desensitization is complete).

Anesthetic modulation of agonist-induced currents

The effect of anesthetics on the response to a pulse of agonist of duration τ has most commonly been explored in one of two general protocols: coapplication of the two solutes (i.e., $c_{an} = 0$ for $t < 0$ and $t > \tau$) or in the continuous presence of anesthetic at concentration c_{an}, i.e., before, during and after the agonist pulse. Predicted traces of both types are considered next.

Coapplied anesthetic

Various concentration ranges of agonist and the anesthetic isoflurane (as well as sevoflurane, xenon and nitrous oxide) have been explored (11–14,19).

For the very low agonist concentrations discussed in the section "Very low c_{ag}" above (i.e., for which the peak current is no more than 20% or so of the maximum, and the current rises monotonically to its steady-state value), coapplication of the anesthetic isoflurane has multiple effects, as shown in Fig. 3 *a* for $c_{ag} = K_{d,R}/10 = 16.7\ \mu M$. As c_{an} is increased, the peak current increases and is reached more rapidly, and slow desensitization begins to be observed. At this low agonist concentration, the maximum in the peak current occurs at $c_{an} \sim 0.75$ mM. With further increase in c_{an}, the peak current drops but continues to be reached more rapidly; the extent and rate of desensitization are predicted to increase as well. By $c_{an} \approx 5$ mM, the desensitization has become extremely fast. As was the case for the anesthetic-only traces described earlier, a rebound current upon washout is predicted. This overall behavior agrees with observations for isoflurane (11) and sevoflurane (14).

The acceleration to the peak and initial increase in its magnitude arise largely from the rapid increase in $k_{A_2R \to A_2O}$ with increasing c_{an}. At higher c_{an}, the decrease in the peak is due largely to the enormous acceleration of branched desensitization ($A_2R \rightarrow A_2D$), whereas the increase in extent of desensitization arises largely from the very positive value of $\alpha_{an,D \to O}$, which shifts the $A_2O \rightleftarrows A_2D$ equilibrium toward the D state.

At higher c_{ag} corresponding to binding saturation ($c_{ag} > K_{d,R}$), an example of which is shown in Fig. 3 *b*, the effect of increasing c_{an} is predicted to differ somewhat from its effect at lower c_{ag}. The c_{an}-dependence of the rebound current is similar to what is predicted at subsaturating c_{ag}. Both the rate and the extent of desensitization increase with c_{an}; the peak open fraction, which is large at low c_{an}, decreases significantly at sufficiently high c_{an}. Although two of the effects of the increasing c_{an}—the increased extent of desensitization and decreased initial peak—agree with observations for isoflurane and sevoflurane (11,14), the *shape* of the predicted desensitization differs significantly from some of the experimental traces. For example, in the experimental traces in Fig. 1 in Neumahr et al. (11), and Fig. 3 in Hapfelmeier et al. (14), increasing c_{an} results in growth of a fast initial component to desensitization, but does *not* significantly alter the time constant of slow desensitization. In contrast, the model does *not* predict the appearance of a fast component but predicts a gradual acceleration in the overall rate of desensitization. We note that other experimental results are in closer agreement to the predictions of our model; for example, a study on isoflurane effects on GABA channels in crayfish (20) does exhibit a gradual increase in the rate of desensitization with increasing c_{an}, at $c_{ag} = 10$ mM, without the development of a fast component.

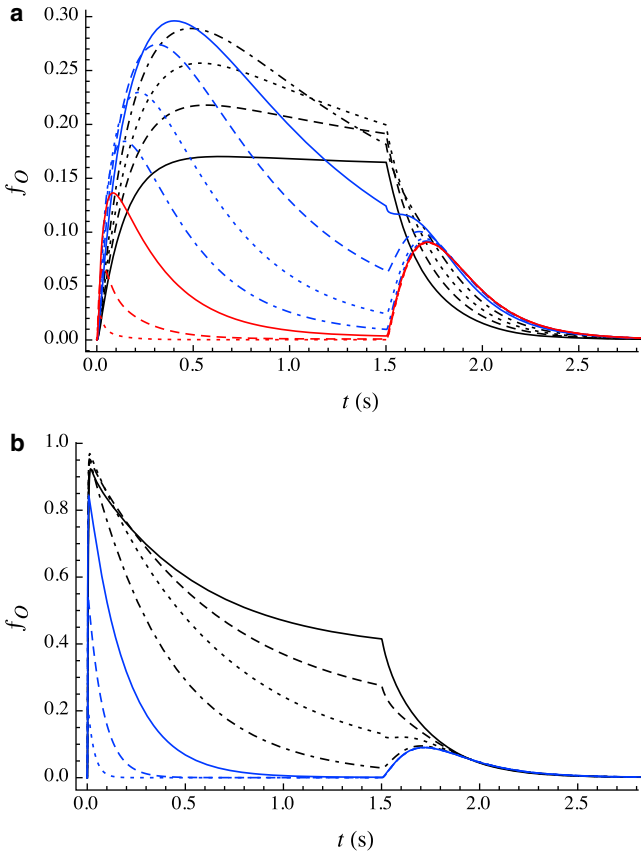

FIGURE 3 Predicted open fraction $f_O(t)$ for a 1.5 s pulse of coapplied agonist and isoflurane. (*a*) $c_{ag} = 0.1K_{d,R} = 16.7\ \mu M$; $c_{an} = 0$ mM (*black line*), 0.15 mM (*black dashed line*), 0.3 mM (*black dotted line*), 0.5 mM (*black dot-dashed line*), 0.75 mM (*blue line*), 1.0 mM (*blue dashed line*), 1.25 mM (*blue dotted line*), 1.6 mM (*blue dot-dashed line*), 2.2 mM (*red line*), 3 mM (*red dashed line*), and 5 mM (*red dotted line*). (*b*) $c_{ag} = 6K_{d,R} = 1.0$ mM; $c_{an} = 0$ mM (*black line*), 0.2 mM (*black dashed line*), 0.7 mM (*black dotted line*), 1.6 mM (*black dot-dashed line*), 3 mM (*blue line*), 6 mM (*blue dashed line*), and 15 mM (*blue dotted line*). To see this figure in color, go online.

Given these differences, it is important to consider the origin of the predicted acceleration in desensitization, i.e., in the net flow of probability from A_2O to A_2D. It arises because anesthetic adsorption shifts the predominant pathway from direct ($A_2O \rightarrow A_2D$) to indirect ($A_2O \rightleftarrows A_2R \rightarrow A_2D$.) Consider the indirect pathway: at low c_{an}, $k_{A_2R \to A_2D} \approx k^{\circ}_{A_2R \to A_2D}$ is small, and the prior quasi-equilibrium of the two opposing faster steps $A_2O \rightleftarrows A_2R$ strongly

favors A_2O, so the overall rate constant for the indirect pathway is $k^{\circ}_{\text{indirect}} \approx (k^{\circ}_{A_2O \to A_2R}/k^{\circ}_{A_2R \to A_2O})k^{\circ}_{A_2R \to A_2D} \approx .03\ s^{-1}$, i.e., it makes negligible contribution to desensitization. So, in the absence of anesthetic adsorption, desensitization is governed by the direct route, since $k_{\text{direct}} \approx k^{\circ}_{A_2O \to A_2D} + k^{\circ}_{A_2D \to A_2O} \gg k_{\text{indirect}}$. Adsorption of anesthetic results in acceleration of $A_2R \to A_2D$ ($\alpha_{R \to D} = -14.4$) and $A_2R \to A_2O$ (although to a lesser degree; $\alpha_{R \to O} = -9.1$), the net effect of which is an increase in $k_{\text{indirect}} \approx (k_{A_2O \to A_2R}/k_{A_2R \to A_2O})k_{A_2R \to A_2D}$ that ultimately exceeds k_{direct}, the indirect route thus becoming the dominant pathway of desensitization.

Fig. 4 compares traces evoked by coapplied agonist and isoflurane at extremely high c_{an} (= 15 mM) as a function of c_{ag}. The size of the rebound peak increases from ~0.03 at $c_{ag} = 0$ to ~0.09 at $c_{ag} = 5\ \mu M$ and remains at this value with increasing c_{an}. This increase in peak height occurs over a narrow range of very low (submicromolar) concentrations. The peak shape, and the concentration at which its height increases (~0.1 μM) is in agreement with experimental traces, as seen in Fig. 3B in Hapfelmeier et al. (12). However, the magnitude of the predicted increase in the rebound peak is significantly less than observed experimentally.

This growth of the rebound peak is readily understood in the context of the model. At the end of the pulse, virtually all of the protein is in the D conformation. For $c_{ag} < K_{d,R}$, it is predominantly unliganded, whereas for $c_{ag} > K_{d,R}$, it is diliganded. Regardless of ligation, anesthetic desorption occurs on a faster timescale ($k_{off,an} = 320\ s^{-1}$) than either agonist dissociation or conformational transitions from the

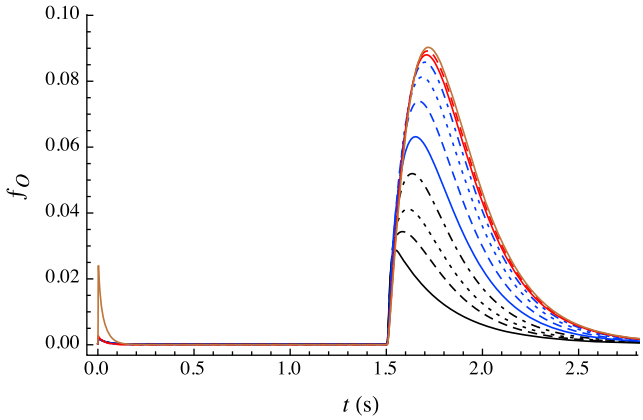

FIGURE 4 Predicted open fraction $f_O(t)$ for a 1.5 s pulse of coapplied agonist and isoflurane; all at the same extremely *high* anesthetic concentration (c_{an} = 15 mM) but with varying (extremely *low*) agonist concentrations: c_{ag} = 0 μM (*black line*), 0.02 μM (*black dashed line*), 0.04 μM (*black dotted line*), 0.08 μM (*black dot-dashed line*), 0.15 μM (*blue line*), 0.3 μM (*blue dashed line*), 0.6 μM (*blue dotted line*), 1.25 μM (*blue dot-dashed line*), 2.5 μM (*red line*), 5 μM (*red dashed line*), and 100 μM (*brown line*). The rebound peak reaches its maximum at ~5 μM. As is evident in the predicted trace at c_{ag} = 100 μM, an initial peak current is predicted to develop (with no effect on the rebound) and continues to grow as c_{ag} is further increased (not shown), as observed experimentally (e.g., see Fig. 3B in 12). To see this figure in color, go online.

A_iD state. The path back from A_iD to A_0R thus occurs largely under the influence of the standard rate constants. For the unliganded case (as discussed earlier for anesthetic-induced traces), upon washout, the path back from A_0D to A_0R is predominantly via the direct route, because $k^{\circ}_{A_0D \to A_0R} (\approx 85\ s^{-1}) \gg k^{\circ}_{A_0D \to A_0O} (\approx 3.8\ s^{-1})$, and thus the rebound peak is small ($f_{O,peak} \approx 0.03$). However, for the diliganded case the other processes dominate, because $k^{\circ}_{A_2D \to A_2R} (= 0.022\ s^{-1})$ is so small. The higher value of $f_{O,peak}$ ($\approx$0.09) arises largely from two routes to the open state: $A_2D \to A_2O$ and $A_2D \to A_1D + A \to A_1O$. The peak remains small in absolute terms, however, because other paths from A_2D to A_0R that do not involve the open state still prevail overall, largely through $A_2D \to A_1D + A \to A_1R + A \to A_0R + 2A$, or $A_2D \to A_0D + 2A \to A_0R + 2A$. The timescale of the decay is determined largely from the closing transitions $A_iO \to A_iR$; because there are significant contributions from all three ligation states (i = 0, 1, 2), with rate constants spread from 2.8 s^{-1} to 26.7 s^{-1}, the decay is not well fit by a single exponential.

Continuous application of anesthetic

All the cases discussed above involve coapplication of anesthetic with agonist during the pulse. However, it is important to examine as well the effect of the continuous presence of an anesthetic (i.e., before, during and after the agonist pulse) on the response of $GABA_A$ receptors to a very short pulse of agonist at saturating concentrations. Aside from providing an additional test of the model, the latter protocol far more closely mimics the effect of anesthetics on inhibitory postsynaptic currents. Two general trends are typically observed for volatile anesthetics such as isoflurane (13,16,17; R. Haseneder, unpublished data) although the details vary significantly with $GABA_A$ subunit composition (17). With increasing isoflurane concentration 1) the initial peak current remains approximately constant up to clinical concentrations (MAC), beyond which it drops rapidly, and 2) the timescale of deactivation lengthens, even at very low c_{an}, reaching a maximum at ~1 mM $\approx$ 3 MAC (17,21). These two trends have opposing effects on the total ion flow Q (integrated current), which thus rises from its value in the absence of anesthetic to a maximum at supraclinical concentrations and decreases thereafter (21). Traces predicted from the kinetic model are shown in Fig. 5 *a* for a short pulse at saturating c_{ag}, over a broad range of anesthetic concentrations. The total ion flow relative to its value in the absence of anesthetic, $Q(c_{an})/Q(0)$ is graphed in Fig. 5 *b*, along with the value of the peak open fraction relative to its value in the absence of anesthetic, $f_{O,peak}(c_{an})/f_{O,peak}(0)$. In good agreement with the experimental results cited above, the slowing of deactivation is already evident at clinical concentrations of anesthetic. The total ion flow thus rises with c_{an}, increasing by a factor of two at $c_{an} \approx$ 1 mM, although the peak current is beginning to decrease.

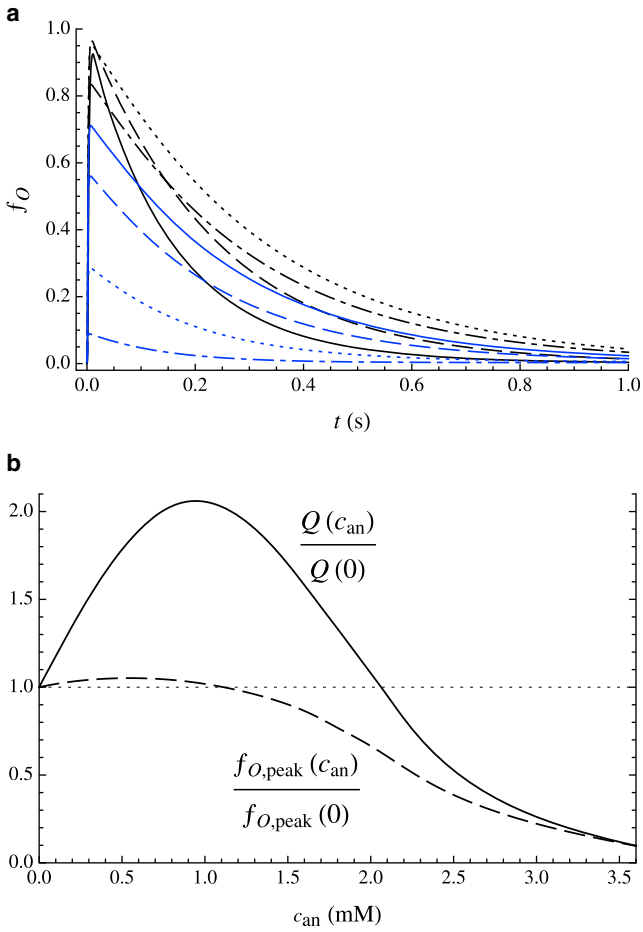

FIGURE 5 (*a*) Response to a short pulse (10 ms) of agonist ($c_{ag} = 10K_{d,R} =$ 1.67 mM), for varying continuous concentration of anesthetic: $c_{an} = 0$ (*black line*), 0.3 mM (*black dashed line*), 0.9 mM (*black dotted line*), 1.5 mM (*black dot-dashed line*), 1.8 mM (*blue line*), 2.1 mM (*blue dashed line*), 2.7 mM (*blue dotted line*), and 3.6 mM (*blue dot-dashed line*). (*b*) Solid curve, $Q(c_{an})/Q(0)$: dependence of total ion flow (integrated current) on c_{an}, relative to total ion flow for $c_{an} = 0$. Dashed curve, $f_{O,peak}(c_{an})/f_{O,peak}(0)$: dependence of peak open fraction on c_{an}, relative to peak open fraction for $c_{an} = 0$. To see this figure in color, go online.

With further increase in c_{an}, the peak current drops dramatically. In the context of the model, the reduction in peak current results from the anesthetic-induced shift in the equilibrium between the A_0R and A_0D states (prior to the agonist pulse) as evident in Fig. 1 *b*. In the range of roughly 1 to 2 mM, although the peak current is reduced, the total ion flow is still larger than in the absence of anesthetic.

DISCUSSION

Approximations

The effect of solute adsorption on the free energy landscape is modeled using two simplistic approximations. In the Langmuir approximation, the partitioning between the aqueous and bilayer phases is quantified by treating the bilayer essentially as a single (effectively two-dimensional) unstructured layer onto which solutes adsorb, with adsorbed molecules interacting only through excluded volume. The quality of this approximation is likely to worsen with increasing surface densities, both because solutes may adsorb over a range of depths in the bilayer, with different kinetic and thermodynamic characteristics, and because there may be strong interactions among adsorbed solutes. The second approximation is that the effect on the free energy landscape of an adsorbed solute is linear in its surface density (Eq. 1), which may be inaccurate if adsorption alters the physical properties of the bilayer itself. Although valid at low adsorption, both of these approximations are likely to become increasingly inaccurate at high levels of adsorption. Unfortunately, it is not yet possible to improve on these approximations, because relevant experimental data (such as the bilayer adsorption isotherm of each solute) are not presently available.

Parameter set

The parameters were chosen to reproduce reasonably well a broad range of electrophysiological traces. Although we found no evidence of any other set of parameters that could provide such broad qualitative agreement, a comprehensive search to eliminate such possibilities would be virtually impossible. However, the important conclusion is that it is indeed possible to reproduce the full range of features of these traces using this model, and that some of the key parameters, such as $k_{off,ag}$ and $k_{off,an}$, are directly related to model-independent experimental measurements, and could thus serve as a definitive test of the model. Although the values of bilayer desorption rate constants for isoflurane and GABA have not been reported, the predicted values, $k_{off,isoflurane} \approx 320$ and $k_{off,GABA} \approx 40$, certainly fall in the range (10 to 1000 s^{-1}) of the compounds for which transport-limited desorption rate constants have been obtained or estimated, as discussed elsewhere (10).

It is useful to examine patterns among the values of the predicted sensitivities, $\alpha_{s,X\to Y}$. For three of the six transitions ($O\to D$, $O\to R$, and $D\to R$) the magnitudes of the sensitivities are very small, both for agonist and anesthetic. On the other hand, the sensitivities are of large magnitude for both $R\to O$ and $R\to D$, although of *opposite signs for the two solutes*: negative for isoflurane and positive for GABA. Only for $\alpha_{s,D\to O}$, is there a significant difference in the magnitude for agonist and anesthetic. These correlations could perhaps be interpreted if it were known which bilayer property might be responsible for coupling of bilayer composition to changes in protein free energy, and how that property depends on the identity of the adsorbed solute. If agonist and anesthetic have closely related effects on this property (although perhaps to a different degree per mole fraction of solute in the bilayer), then the values of the sensitivities might be expected to scale by a single multiplicative constant. For example, it has been suggested (22,23)

that it is the depth-dependent distribution of lateral pressures within the bilayer that couples to the protein free energy landscape. Anesthetics reside predominantly near the aqueous interfaces, where they increase lateral pressures, resulting largely from excluded volume effects, and thus decrease lateral pressures in the bilayer interior; this results in an increase in lipid area and a decrease in bilayer thickness. If, when adsorbed to the bilayer surface, agonists such as GABA or glycine interact principally through electrostatics and hydrogen bonds to lipid head groups, they may well *reduce* inter-head group repulsions, and thus reduce the lateral pressure in that region. If so, then the effects of anesthetics and agonist on the free energy landscape would be expected to have opposite signs, resulting in opposite signs of $\alpha_{ag,X\rightarrow Y}$ and $\alpha_{an,X\rightarrow Y}$, as predicted in the kinetic analysis.

In light of the relatively large number of parameters in our kinetic model, it is useful to consider the minimum number of parameters that would be required for the alternative approach, i.e., a direct binding kinetic scheme, in which both anesthetic and agonist interact with the receptor only by binding to specific sites. As noted earlier, 14 of the 28 parameters in our model—four ligand unbinding/binding and 10 standard rate constants of conformational transitions—depend only on the protein and the binding of its agonist, and would thus need to be specified for *any* three-state model of receptors that includes both linear and branched desensitization. Inclusion of additional conformational states in the scheme—necessary to reproduce key features of agonist-induced traces, such as multiple timescales of desensitization—would require a minimum of five more parameters per additional state, *without yet having considered the effects of anesthetics*. Even for the simplest case in which an anesthetic binds only to a single site on the receptor, specification of a minimum of 12 additional rate constants would be required for the three-state system (26 parameters, total) and 20 additional constants for the four-state system (34, total) as illustrated by the representative scheme in Fig. S3. However, even the latter would almost certainly be insufficiently robust to account either for agonist-only behavior, or for its modulation by anesthetics, for two reasons. First, as discussed in the introduction, kinetic models of agonist-induced currents (2–7) have typically required *two* additional desensitizated states (and often additional open states) to reproduce experimental traces. Second, anesthetics are known to affect current traces over a significantly larger range of concentrations than can be accounted for by a single binding site, so any truly *comprehensive* binding model would require multiple anesthetic binding site(s) of significantly different affinities; the same can be argued for agonist as well. The total number of parameters for a binding model that could account for the full range of features of agonist-induced, anesthetic-induced and anesthetic modulation of agonist-induced traces would thus be vastly in excess of the 28 required in our kinetic model.

What can be concluded from this study of the kinetic mechanism of volatile anesthetic modulation of ion channel activity? Recent studies (24) have indeed identified various locations in which an inhalation (desflurane) and an intravenous (propofol) anesthetic have co-crystallized with prokaryotic members of the pLGIC family, generally interpreted as providing strong support in favor of a direct binding mechanism of their anesthetic action. However, binding affinities (and thus their potential relevance to anesthesia) have not been measured for these sites. More generally, identification of such sites doesn't rationalize the Meyer-Overton correlation over the remarkably broad range of molecular characteristics (size, polarity, shape, flexibility, etc.) of inhalation anesthetics or its well-known exceptions. With regard to these exceptions—most notably the lack of anesthetic potency of nonimmobilizers—it should be noted that results of the essential negative control experiment, co-crystallization of the receptor with a nonimmobilizer, have not been reported. Additionally, within the context of a binding model, it seems difficult to explain the remarkably narrow range of sensitivities to a given anesthetic within the human population: what is the essential process imitated by anesthetics with such minimal molecular specificity that generates such enormous selection pressure? One plausible idea that has been suggested (25) is that the small cavities ubiquitous to many membrane proteins may be essential to facilitate conformational changes that involve (for example) motions of adjacent alpha helices in transmembrane bundles; by occupying these sites, which could presumably accommodate a wide range of small molecules, anesthetics could impede these motions and thereby influence protein function. However, at least for $GABA_A$ receptors, the effect of anesthetics in electrophysiological studies, as modeled in this work, is to *accelerate* conformational transitions, as has been discussed elsewhere (8). Also, although this suggestion could certainly account for the breadth of molecular characteristics among anesthetics, it does not rationalize the Meyer-Overton correlation of anesthetic potency with bilayer partitioning, if the sizes and shapes of these cavities are not critical for endogenous function.

In any case, no kinetic model in which agonist and anesthetics interact with receptors entirely through binding to localized sites, has yet been proposed that can reproduce the full range of effects of anesthetics (over a broad range of anesthetic and agonist concentrations) on electrophysiological traces; this is not surprising in the context of the above discussion. By contrast, the kinetic model discussed in this article can not only reproduce the diverse features of electrophysiological traces (and does so with only three protein conformational states) but involves key parameters that can be determined through model-independent experimental measurements. And as discussed elsewhere (10), in the context of the bilayer lateral pressure profile it not only explains the Meyer-Overton correlation but it correctly predicts known exceptions, such as the cutoff in potency in

long-chain n-alkanols (26), and predicted the anesthetic potency of long-chain polyhydric alkanols—unexpected in the context of a binding model, given the very large volume of those compounds—that was subsequently demonstrated experimentally (27). Finally, since details of temporal modulation of receptor activity—desensitization and deactivation—appear to be important (or perhaps even essential) for proper protein function, if these characteristics result from (nonspecific) adsorption of neurotransmitter to the bilayer, then the model provides a plausible explanation of the strong apparent selection pressure for correct anesthetic sensitivity (10,28), and predicted that noncognate neurotransmitters would significantly modulate receptor activity, as subsequently demonstrated experimentally (29).

SUPPORTING MATERIAL

Three figures, two tables, and a Mathematica notebook are available at http://www.biophysj.org/biophysj/supplemental/S0006-3495(15)00060-0.

AUTHOR CONTRIBUTIONS

Both D.K.L. and D.J.A. developed software, contributed to model development, and performed extensive kinetic analysis. R.S.C. designed the model, developed software, performed kinetic modeling and analysis, and wrote this article.

ACKNOWLEDGMENTS

We thank Jim Sonner for provocative discussions and many valuable suggestions.

REFERENCES

1. Jones, M. V., and G. L. Westbrook. 1995. Desensitized states prolong $GABA_A$ channel responses to brief agonist pulses. *Neuron.* 15:181–191.
2. Burkat, P. M., J. Yang, and K. J. Gingrich. 2001. Dominant gating governing transient GABA(A) receptor activity: a first latency and Po/o analysis. *J. Neurosci.* 21:7026–7036.
3. Celentano, J. J., and A. G. Hawkes. 2004. Use of the covariance matrix in directly fitting kinetic parameters: application to $GABA_A$ receptors. *Biophys. J.* 87:276–294.
4. Celentano, J. J., and R. K. Wong. 1994. Multiphasic desensitization of the $GABA_A$ receptor in outside-out patches. *Biophys. J.* 66:1039–1050.
5. Haas, K. F., and R. L. Macdonald. 1999. $GABA_A$ receptor subunit gamma2 and delta subtypes confer unique kinetic properties on recombinant $GABA_A$ receptor currents in mouse fibroblasts. *J. Physiol.* 514:27–45.
6. Lema, G. M. C., and A. Auerbach. 2006. Modes and models of $GABA_A$ receptor gating. *J. Physiol.* 572:183–200.
7. Milescu, L. S., G. Akk, and F. Sachs. 2005. Maximum likelihood estimation of ion channel kinetics from macroscopic currents. *Biophys. J.* 88:2494–2515.
8. Cantor, R. S., K. Twyman, …, R. Haseneder. 2009. A kinetic model of ion channel electrophysiology: bilayer-mediated effects of agonists and anesthetics on protein conformational transitions. *Soft Matter.* 5:3266–3278.
9. Haseneder, R., G. Rammes, …, G. Hapfelmeier. 2002. $GABA_A$ receptor activation and open-channel block by volatile anaesthetics: a new principle of receptor modulation? *Eur. J. Pharmacol.* 451:43–50.
10. Sonner, J. M., and R. S. Cantor. 2013. Molecular mechanisms of drug action: an emerging view. *Annu. Rev. Biophys.* 42:143–167.
11. Neumahr, S., G. Hapfelmeier, …, E. Kochs. 2000. Dual action of isoflurane on the γ-aminobutyric acid (GABA)-mediated currents through recombinant $\alpha_1\beta_2\gamma_{2L}$-$GABA_A$-receptor channels. *Anesth. Analg.* 90: 1184–1190.
12. Hapfelmeier, G., R. Haseneder, …, W. Zieglgänsberger. 2001. Coadministered nitrous oxide enhances the effect of isoflurane on GABAergic transmission by an increase in open-channel block. *J. Pharmacol. Exp. Ther.* 298:201–208.
13. Hapfelmeier, G., R. Haseneder, …, W. Zieglgänsberger. 2001. Isoflurane slows inactivation kinetics of rat recombinant $\alpha_1\beta_2\gamma_{2L}$ $GABA_A$ receptors: enhancement of GABAergic transmission despite an open-channel block. *Neurosci. Lett.* 307:97–100.
14. Hapfelmeier, G., H. Schneck, and E. Kochs. 2001. Sevoflurane potentiates and blocks GABA-induced currents through recombinant $\alpha_1\beta_2\gamma_2$ $GABA_A$ receptors: implications for an enhanced GABAergic transmission. *Eur. J. Anaesthesiol.* 18:377–383.
15. Krampfl, K., J. Bufler, …, H. Adelsberger. 2000. Desensitization characteristics of rat recombinant $GABA_A$ receptors consisting of $\alpha_1\beta_2\gamma_{2S}$ and $\alpha_1\beta_2$ subunits expressed in HEK293 cells. *Neurosci. Lett.* 278: 21–24.
16. Jones, M. V., and N. L. Harrison. 1993. Effects of volatile anesthetics on the kinetics of inhibitory postsynaptic currents in cultured rat hippocampal neurons. *J. Neurophysiol.* 70:1339–1349.
17. Benkwitz, C., M. I. Banks, and R. A. Pearce. 2004. Influence of $GABA_A$ receptor γ_2 splice variants on receptor kinetics and isoflurane modulation. *Anesthesiology.* 101:924–936.
18. Mercik, K., E. D. Zarnowska, …, J. W. Mozrzymas. 2002. Saturation and self-inhibition of rat hippocampal $GABA_A$ receptors at high GABA concentrations. *Eur. J. Neurosci.* 16:2253–2259.
19. Hapfelmeier, G., W. Zieglgänsberger, …, E. Kochs. 2000. Nitrous oxide and xenon increase the efficacy of GABA at recombinant mammalian $GABA_A$ receptors. *Anesth. Analg.* 91:1542–1549.
20. Adelsberger, H., J. Wilde, …, J. Dudel. 1998. Multiple mechanisms of block by the anesthetic isoflurane of a γ-aminobutyric acid activated chloride channel in crayfish. *J. Comp. Physiol. A Neuroethol. Sens. Neural Behav. Physiol.* 182:51–58.
21. Banks, M. I., and R. A. Pearce. 1999. Dual actions of volatile anesthetics on $GABA_A$ IPSCs. *Anesthesiology.* 90:120–134.
22. Cantor, R. S. 1997. The lateral pressure profile in membranes: a physical mechanism of general anesthesia. *Biochemistry.* 36:2339–2344.
23. Cantor, R. S. 1999. The influence of membrane lateral pressures on simple geometric models of protein conformational equilibria. *Chem. Phys. Lipids.* 101:45–56.
24. Nury, H., C. Van Renterghem, …, P.-J. Corringer. 2011. X-ray structures of general anaesthetics bound to a pentameric ligand-gated ion channel. *Nature.* 469:428–431.
25. Eckenhoff, R. G. 2008. Why can all of biology be anesthetized? *Anesth. Analg.* 107:859–861.
26. Cantor, R. S. 2001. Breaking the Meyer-Overton rule: predicted effects of varying stiffness and interfacial activity on the intrinsic potency of anesthetics. *Biophys. J.* 80:2284–2297.
27. Mohr, J. T., G. W. Gribble, …, R. S. Cantor. 2005. Anesthetic potency of two novel synthetic polyhydric alkanols longer than the n-alkanol cutoff: evidence for a bilayer-mediated mechanism of anesthesia? *J. Med. Chem.* 48:4172–4176.
28. Cantor, R. S. 2003. Receptor desensitization by neurotransmitters in membranes: are neurotransmitters the endogenous anesthetics? *Biochemistry.* 42:11891–11897.
29. Milutinovic, P. S., L. Yang, …, J. M. Sonner. 2007. Anesthetic-like modulation of a γ-aminobutyric acid type A, strychnine-sensitive glycine, and N-methyl-D-aspartate receptors by coreleased neurotransmitters. *Anesth. Analg.* 105:386–392.

Supporting Materials

D.K. Lee, D.J. Albershardt, and R.S. Cantor. "Exploring the mechanism of general anesthesia: Kinetic analysis of $GABA_A$ receptor electrophysiology"

Two Tables and three Figures are provided below. In addition, animation software is available for download that dynamically illustrates the time-dependent flow of probability among protein states in the kinetic scheme. It runs interactively, allowing the user to vary the three experimental parameters: c_{ag} (agonist concentration), c_{an} (anesthetic concentration), and τ (pulse duration). The user can select whether the anesthetic is coapplied with agonist during the pulse, or is continuously present. This file, "KineticSchemeAnimation.nb", requires either Mathematica™ or PlayerPro™ (Wolfram Research, Inc., Champaign, IL) to be run.

Table S1. Parameter set. The values of model parameters used in generating the predicted traces, chosen to reproduce the features of current traces (9, 11-13) for recombinant $\alpha_1\beta_2\gamma_{2L}$ $GABA_A$ receptors and the anesthetic isoflurane, over a broad range of agonist and isoflurane concentrations. A set of 28 independent parameters is indicated in **boldface** on the left; the parameters on the right are derived as indicated from this set. Of the 28, the 14 rate constants of agonist binding (a) and conformational transitions (b) depend only on the protein, i.e., they are independent of any effects of bilayer adsorption. In contrast, the bilayer adsorption/desorption rate constants (c) depend only on the solute (agonist or anesthetic) and the bilayer, i.e., they are independent of the protein. The sensitivities (d, e) depend both on the protein and on bilayer-mediated effects. Note that only three of the independent parameters $\{K_{d,R}, K_{ads,ag}, K_{ads,an}\}$ involve concentrations; the rest are either first-order rate constants or dimensionless. Transition rate constants of monoliganded protein are the geometric mean of the corresponding constants for unliganded and diliganded protein, i.e., $k_{A_1X\to A_1Y} = (k_{A_0X\to A_0Y}\, k_{A_2X\to A_2Y})^{1/2}$.

(a) Agonist binding/unbinding:

$\boldsymbol{k_{u,R}} = \mathbf{100\ s^{-1}}$	$\boldsymbol{K_{d,R}} = \mathbf{167\ \mu M}$	$k_{b,R} = k_{u,R} / K_{d,R} = 0.6\times10^6\ M^{-1}\ s^{-1}$
$\boldsymbol{k_{u,O}} = \mathbf{0.40\ s^{-1}}$		$K_{d,O} = K_{d,R}\,(K°_{open,2}/K°_{open,0})^{1/2} = 0.52\ \mu M$
		$k_{b,O} = k_{u,O} / K_{d,O} = 0.77\times10^6\ M^{-1}\ s^{-1}$
$\boldsymbol{k_{u,D}} = \mathbf{4.0\ s^{-1}}$		$K_{d,D} = K_{d,R}\,(K°_{desbr,2}/K°_{desbr,0})^{1/2} = 0.20\ \mu M$
		$k_{b,D} = k_{u,D} / K_{d,D} = 2.0\times10^6\ M^{-1}\ s^{-1}$

(b) Conformational transitions; standard rate and equilibrium constants:

Opening/closing:

$\boldsymbol{k°_{A_0R\rightarrow A_0O} = 8.1\times10^{-4}\ s^{-1}}$ $\boldsymbol{K°_{open,0} = 2.9\times10^{-4}}$ $k°_{A_0O\rightarrow A_0R} = k°_{A_0R\rightarrow A_0O}/K°_{open,0} = 2.8\ s^{-1}$

$\boldsymbol{k°_{A_2R\rightarrow A_2O} = 800\ s^{-1}}$ $\boldsymbol{K°_{open,2} = 30}$ $k°_{A_2O\rightarrow A_2R} = k°_{A_2R\rightarrow A_2O}/K°_{open,2} = 26.7\ s^{-1}$

Linear desensitization/resensitization:

$\boldsymbol{k°_{A_0O\rightarrow A_0D} = 0.84\ s^{-1}}$ $\boldsymbol{K°_{deslin,0} = 0.22}$ $k°_{A_0D\rightarrow A_0O} = k°_{A_0O\rightarrow A_0D}/K°_{deslin,0} = 3.82\ s^{-1}$

$\boldsymbol{k°_{A_2O\rightarrow A_2D} = 1.1\ s^{-1}}$ $\boldsymbol{K°_{deslin,2} = 1.5}$ $k°_{A_2D\rightarrow A_2O} = k°_{A_2O\rightarrow A_2D}/K°_{deslin,2} = 0.73\ s^{-1}$

Branched desensitization/resensitization:

$\boldsymbol{k°_{A_0R\rightarrow A_0D} = 5.4\times10^{-3}\ s^{-1}}$ $K°_{desbr,0} = K°_{open,0}\ K°_{deslin,0} = 6.4\times10^{-5}$

$k°_{A_0D\rightarrow A_0R} = k°_{A_0R\rightarrow A_0D}/K°_{desbr,0} = 84.6\ s^{-1}$

$\boldsymbol{k°_{A_2R\rightarrow A_2D} = 1.0\ s^{-1}}$ $K°_{desbr,2} = K°_{open,2}\ K°_{deslin,2} = 45.0$

$k°_{A_2D\rightarrow A_2R} = k°_{A_2R\rightarrow A_2D}/K°_{desbr,2} = 0.022\ s^{-1}$

(c) Solute adsorption/desorption to bilayer (anesthetic = isoflurane):

$\boldsymbol{k_{off,an} = 320\ s^{-1}}$ $\boldsymbol{K_{ads,an} = (2\ mM)^{-1}}$ $k_{on,an} = k_{off,an}\ K_{ads,an} = 1.6\times10^{5}\ M^{-1}\ s^{-1}$

$\boldsymbol{k_{off,ag} = 40\ s^{-1}}$ $\boldsymbol{K_{ads,ag} = (10\ mM)^{-1}}$ $k_{on,ag} = k_{off,ag}\ K_{ads,ag} = 4.0\times10^{3}\ M^{-1}\ s^{-1}$

(d) Sensitivities to agonist (GABA):

$\boldsymbol{\alpha_{ag,R\rightarrow O} = 6.0}$ $\boldsymbol{\alpha_{ag,O\rightarrow R} = -1.0}$ $\alpha_{ag,open} = \alpha_{ag,R\rightarrow O} - \alpha_{ag,O\rightarrow R} = 7.0$

$\boldsymbol{\alpha_{ag,O\rightarrow D} = 0.0}$ $\boldsymbol{\alpha_{ag,D\rightarrow O} = 0.5}$ $\alpha_{ag,deslin} = \alpha_{ag,O\rightarrow D} - \alpha_{ag,D\rightarrow O} = -0.5$

$\boldsymbol{\alpha_{ag,R\rightarrow D} = 6.4}$ $\alpha_{ag,D\rightarrow R} = -0.1$ $\alpha_{ag,desbr} = \alpha_{ag,R\rightarrow D} - \alpha_{ag,D\rightarrow R} = 6.5$

(e) Sensitivities to anesthetic (isoflurane):

$\boldsymbol{\alpha_{an,R\rightarrow O} = -9.1}$ $\boldsymbol{\alpha_{an,O\rightarrow R} = -2.5}$ $\alpha_{an,open} = \alpha_{an,R\rightarrow O} - \alpha_{an,O\rightarrow R} = -6.6$

$\boldsymbol{\alpha_{an,O\rightarrow D} = -0.4}$ $\boldsymbol{\alpha_{an,D\rightarrow O} = 10.7}$ $\alpha_{an,deslin} = \alpha_{an,O\rightarrow D} - \alpha_{an,D\rightarrow O} = -11.1$

$\boldsymbol{\alpha_{an,R\rightarrow D} = -14.4}$ $\alpha_{an,D\rightarrow R} = 3.3$ $\alpha_{an,desbr} = \alpha_{an,R\rightarrow D} - \alpha_{an,D\rightarrow R} = -17.7$

Table S2. Rate constants. Values of rate constants of conformational transitions $k_{A_iX \rightarrow A_iY}$ at representative levels of bilayer adsorption (θ_{an}, θ_{ag}) and corresponding equilibrium aqueous concentrations (c_{an}, c_{ag}), calculated from

$$k_{A_iX \rightarrow A_iY} = k^{\circ}_{A_iX \rightarrow A_iY} \exp[-(\alpha_{ag,X \rightarrow Y}\, \theta_{ag} + \alpha_{an,X \rightarrow Y}\, \theta_{an})].$$

Rate constants are expressed in s^{-1} units; c_{an} and c_{ag} are expressed in mM units. Values corresponding to he free energy landscapes plotted in Fig. S2 are indicated in bold with corresponding color.

θ_{an}	c_{an}	θ_{ag}	c_{ag}	$k_{A_0R \rightarrow A_0O}$	$k_{A_0O \rightarrow A_0R}$	$k_{A_0O \rightarrow A_0D}$	$k_{A_0D \rightarrow A_0O}$	$k_{A_0R \rightarrow A_0D}$	$k_{A_0D \rightarrow A_0R}$
0	**0**	**0**	**0**	**0.00081**	**2.79**	**0.84**	**3.82**	**0.0054**	**84.6**
.2	.5	0	0	0.00500	4.61	0.91	0.45	0.096	43.7
.25	.67	0	0	0.00788	5.22	0.93	0.263	0.198	37.1
.33	1.0	0	0	0.0168	6.43	0.96	0.108	0.656	28.2
0.5	**2**	**0**	**0**	**0.0766**	**9.75**	**1.03**	**0.0181**	**7.23**	**16.3**
0.67	4	0	0	0.349	14.8	1.10	0.00305	79.7	9.38
0.75	6	0	0	0.746	18.2	1.13	0.00125	265	7.12
0.8	8	0	0	1.17	20.6	1.16	0.000732	544	6.04
0.89	16	0	0	2.64	25.8	1.20	0.000282	1956	4.50

θ_{an}	c_{an}	θ_{ag}	c_{ag}	$k_{A_2R \rightarrow A_2O}$	$k_{A_2O \rightarrow A_2R}$	$k_{A_2O \rightarrow A_2D}$	$k_{A_2D \rightarrow A_2O}$	$k_{A_2R \rightarrow A_2D}$	$k_{A_2D \rightarrow A_2R}$
0	**0**	**0**	**0**	**800**	**26.7**	**1.1**	**0.73**	**1.0**	**0.0222**
0.2	0.5	0	0	4940	45.0	1.19	0.086	17.8	0.0115
0.25	0.67	0	0	7780	49.8	1.22	0.0505	36.6	0.00974
0.33	1	0	0	16600	61.4	1.26	0.0207	122	0.00740
0.5	**2**	**0**	**0**	**75700**	**93.1**	**1.34**	**0.00348**	**1340**	**0.00427**
0.67	4	0	0	345000	141	1.44	0.000585	14760	0.00246
0.8	8	0	0	1160000	197	1.51	0.000140	100700	0.00159
0.89	16	0	0	2610000	246	1.57	0.0000543	362000	0.00118
0	0	0.2	2.5	241	32.6	1.1	0.664	0.278	0.0227
0	0	0.25	3.33	179	34.2	1.1	0.647	0.202	0.0228
0	0	0.33	5	108	37.2	1.1	0.621	0.118	0.0230
0	**0**	**0.5**	**10**	**39.8**	**44.0**	**1.1**	**0.571**	**0.0408**	**0.0233**
0	0	0.67	20	14.7	51.9	1.1	0.525	0.0140	0.0238
0	0	0.8	40	6.58	59.3	1.1	0.492	0.00598	0.0241
0	0	0.89	80	3.86	64.9	1.1	0.470	0.00338	0.0243

Figure S1. Kinetic scheme.

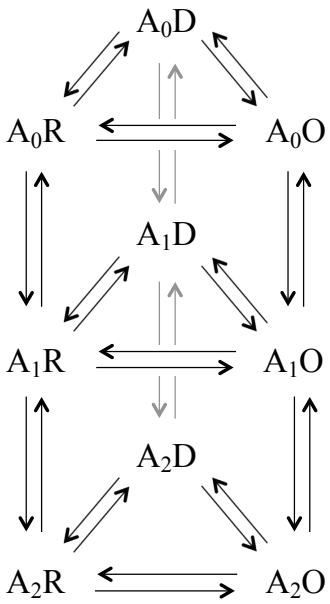

Opening/closing:

$$K_{\text{open,i}} = k_{A_iR \rightarrow A_iO} / k_{A_iO \rightarrow A_iR} \qquad i = \{0, 1, 2\}$$

Linear desensitization/resensitization:

$$K_{\text{deslin,i}} = k_{A_iO \rightarrow A_iD} / k_{A_iD \rightarrow A_iO} \qquad i = \{0, 1, 2\}$$

Branched desensitization/resensitization:

$$K_{\text{desbr,i}} = k_{A_iR \rightarrow A_iD} / k_{A_iD \rightarrow A_iR} \qquad i = \{0, 1, 2\}$$

Agonist unbinding/binding:

$$K_{d,X} = k_{u,X} / k_{b,X} \qquad X = \{R, O, D\}$$

The kinetic scheme includes all nine protein states and the elementary kinetic steps connecting pairs of states. Protein states, labeled A_iX, can exist in one of three conformational states {X = R, O, D}, each of which can be in one of three ligation states $i = \{0, 1, 2\}$, i.e., unliganded, monoliganded or diliganded. Vertical arrows represent agonist binding (down) and unbinding (up) steps; other arrows represent conformational transitions at fixed ligation. Relationships among thermodynamic equilibrium constants (K) and rate constants (k) are listed on the right.

Figure S2. Free energy landscapes.

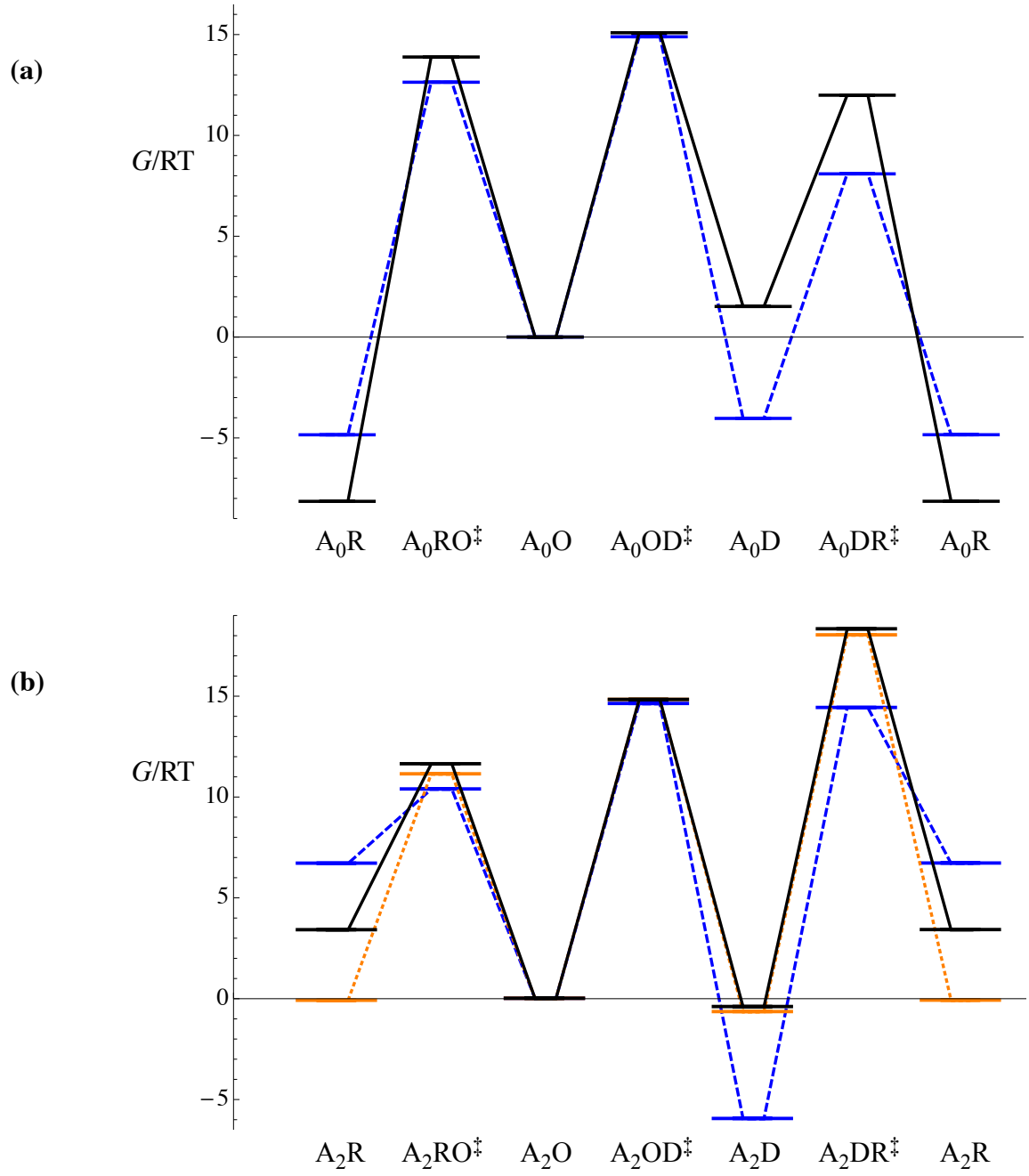

The dimensionless free energy landscape G/RT is plotted for **(a)** unliganded and **(b)** diliganded protein. Black, solid lines: no adsorbed solutes: $\{\theta_{an} = 0, c_{an} = 0;\ \theta_{ag} = 0, c_{ag} = 0\}$. Blue, dashed lines: half-maximal adsorption of anesthetic $\{\theta_{an} = 0.5, c_{an} = K_{ads,an}^{-1} = 2$ mM; $\theta_{ag} = 0, c_{ag} = 0\}$. Orange, dotted lines: half-maximal adsorption of agonist $\{\theta_{an} = 0, c_{an} = 0;\ \theta_{ag} = 0.5, c_{ag} = K_{ads,ag}^{-1} = 10$ mM$\}$. Note that the resting state appears at both the left and right sides of the

plot. The free energies of the conformational and transition states are indicated with horizontal lines; the lines connecting them serve only as a guide to the eye. Note that an additive constant (shift up or down) of any of the landscapes carries no physical significance; only free energy *differences* on a given landscape are meaningful. The relative vertical position of each landscape is thus arbitrary; the zero of free energy for each has arbitrarily been assigned to the open state, irrespective of solute adsorption or agonist ligation.

For a given landscape, the relative positions of the minima (conformational states) are unambiguously determined from the equilibrium constants. However, using the simple Arrenius-like expression from Eq. 2:

$$k_{A_iX \rightarrow A_iY} = A_{A_iX \rightarrow A_iY} \exp\{-\Delta G^{\ddagger}/RT\}, \quad \text{where} \quad \Delta G^{\ddagger} = G(A_iXY^{\ddagger}) - G(A_iX)$$

it is <u>not</u> possible to determine the free energies of the activated complexes, $G(A_iXY^{\ddagger})$, even assuming the pre-exponential factor A to have the same value for all transitions. For purposes of illustration of the effect of adsorption on the free energy of the activated complex, we have assumed a common value of A, one that is large enough to exceed the largest values of any of the rate constants in any of the plotted landscapes (and thus ensure that $\Delta G^{\ddagger} > 0$ for all transitions).

Figure S3.

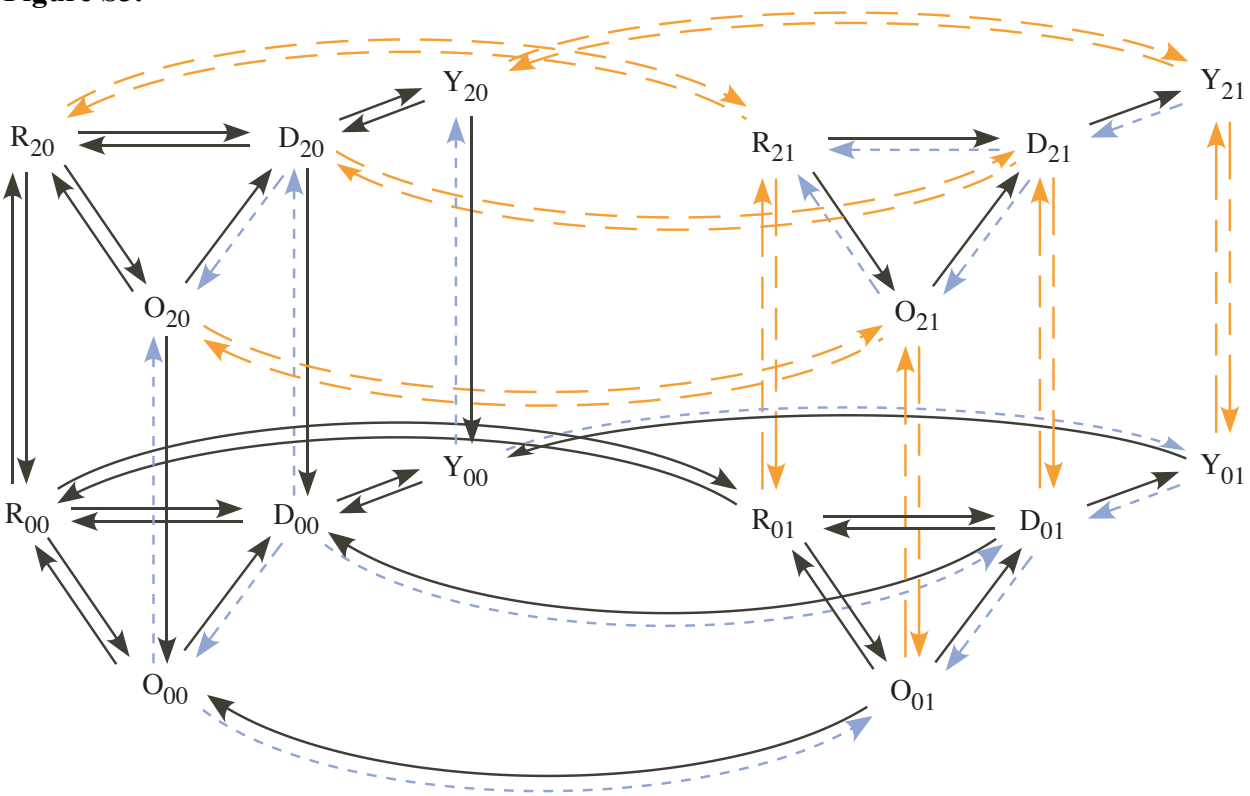

Shown above is a generic kinetic scheme involving only *specific binding* of agonist and anesthetic, for the purpose of determining the minimum number of independent kinetic parameters; this can be compared with the number of parameters (28) of our kinetic model. It assumes a single anesthetic binding site and two equivalent agonist sites. A fourth conformational state "Y" is included, accessed from a single state, arbitrarily chosen to be D. States are labeled X_{ij}, where $i = \{0,1,2\}$ indicates agonist ligation and $j = \{0,1\}$ indicates anesthetic ligation. A complete set of independent parameters is indicated by solid lines for the corresponding binding and transition kinetic steps (the choice is not unique, but the number is fixed.) Dotted lines indicate processes whose rate constants are determined through thermodynamic constraints; dashed lines represent processes whose rate constants are identical to others in the diagram. The rate constant of each conformational transition of the monoliganded protein is assumed to be the geometric mean of the corresponding unliganded and diliganded transitions, and it is also assumed that anesthetic and agonist binding are independent, i.e., the rate constant of agonist binding to conformation X is independent of anesthetic ligation and vice versa. With these assumptions, for the purpose of determining the number of independent parameters, it is thus unnecessary to include the monoliganded states in the diagram (although they would be present and fully incorporated in the kinetics). For this case, with four conformational states, specification of 34 independent parameters would thus be required, the number increasing by a minimum of 8 for each additional conformational state.